Geophys. J. Int. (2008) **172,** 345–362 doi: 10.1111/j.1365-246X.2007.03636.x

Lithospheric structure and deep earthquakes beneath India, the Himalaya and southern Tibet

Keith Priestley, James Jackson and Dan McKenzie

Bullard Laboratories, University of Cambridge, UK. E-mail: keith@madingley.org

Accepted 2007 September 26. Received 2007 July 13; in original form 2007 February 17

SUMMARY

This paper is concerned with the implications of earthquake depth distributions in the Himalayan–Tibetan collision zone for the general understanding of lithosphere rheology. In particular, recent studies have argued that microearthquakes in the uppermost mantle beneath Nepal and some earthquakes at 80–90 km depth, close to the Moho in SE and NW Tibet, reinforce the conventional view of the last 25 yr that the continental lithosphere is well represented by strong seismogenic layers in the upper crust and uppermost mantle, separated by a weak and aseismic lower crust. That view was recently challenged by an alternative one suggesting that the continental lithosphere contained a single strong seismogenic layer, that was either the upper crust or the whole crust, but did not involve the mantle. We re-examine the seismic structure and seismicity of the Himalayan–Tibetan collision zone, recalculating earthquake depths in velocity structures that are consistent with seismic receiver functions and surface wave dispersion studies, and calculating a geotherm for the Indian Shield consistent with kimberlite nodule geochemistry. Earthquakes occur throughout the crustal thickness of the Indian Shield, where the lower crust is thought to consist of dry granulite, responsible for its seismogenic behaviour and strength as manifested by its relatively large effective elastic thickness. The crust of the Indian Shield is thin (∼35 km) for an Archean shield, and this, in turn, leads to a steady-state Moho temperature that could be as low as ∼500 °C. When this shield is thrust beneath the Himalaya in Nepal, the relatively low mantle temperature, together with the high strain rates associated with it adopting a 'ramp-and-flat' geometry, may be responsible for the mantle microearthquakes that accompany other earthquakes in the lower crust. Further north, the upper crust of India south of the Indus Suture Zone has been removed, the uppermost lower crust of India has heated up, and seismicity is restricted to a few earthquakes very close to the Moho at 80–90 km, where errors in Moho and earthquake depth determinations make it unclear whether these events are in the crust or mantle. A similar situation exists in NW Tibet beneath the Kunlun, where earthquakes at 80–90 km depth occur very close to the Moho. Both places are about 400 km north of the Himalayan front, and we suspect both represent the minimum distance India has underthrust Tibet, so that India underlies most of the SE and nearly all of the NW Tibetan plateau. The distribution of earthquake depths throughout the region is consistent with a generic global view of seismicity in which earthquakes occur in (1) 'wet' upper crustal material to a temperature of ∼350 °C, or (2) higher temperatures in dry granulite-facies lower crust or (3) mantle that is colder than ∼600 °C.

Key words: Seismicity and tectonics; Cratons; Crustal structure; Rheology: crust and lithosphere; Rheology: mantle.

1 INTRODUCTION

For over 20 yr the most commonly accepted model for the rheology of the continental lithosphere has been the one proposed by Chen & Molnar (1983), in which the upper crust and uppermost mantle are relatively strong, and the intervening lower crust is relatively weak. The depth distribution of continental earthquakes (e.g. Chen & Molnar 1983) and laboratory studies of rock strength extrapolated to geological conditions (e.g. Brace & Kohlstedt 1980) were used as evidence supporting this model. Although most continental earthquakes occur at shallow depths in the upper crust, Chen & Molnar (1983) pointed to a few locations where there appeared to be two depth-levels of earthquakes beneath the continents, with the bulk of the earthquakes occurring in the upper crust, an aseismic crustal section below, and occasional deeper earthquakes that were assumed to be in the uppermost continental mantle. Chen & Molnar

(1983) noted that the creep strength of rock is primarily a function of homologous temperature. Thus, we expect typical continental thermal gradients will lead to crustal deformation being dominated by frictional (and seismogenic) processes at depths shallower than about 15–20 km, but dominated by creep (and aseismic) processes at deeper depths in the crust, especially in the presence of fluids, which lowers creep strength. The change in mineralogy and probable drop in homologous temperature across the Moho could put the olivine-rich rocks of the uppermost mantle back into the frictional (seismic) regime, especially if they are dry (Brace & Kohlstedt 1980; Mackwell *et al.* 1998). Consequently, Chen & Molnar (1983) took the presence of earthquakes at two levels in the continental lithosphere as evidence that the upper crust and uppermost mantle could support frictional failure and were thus relatively strong, while the apparent absence of earthquakes in the lower crust was support for the view that this part of the continental lithosphere was relatively weak.

This rheological model for the continental lithosphere has recently been re-examined and questioned (Maggi *et al.* 2000a; Jackson 2002a) in the light of much new data on crustal structure and earthquake focal depths that have accumulated in the past 25 yr. A central conclusion of Maggi *et al.* (2000b) and Jackson (2002a) is that a single, all-purpose model of rheology does not fit the geographical variations in seismogenic thickness (T_s) and effective elastic thickness (T_e) that are seen on the continents. They found that, in most continental regions, earthquakes are restricted to the upper crust; a view that has not changed in the last 30 yr. However, in a few regions, mostly associated with Precambrian shields, they found that earthquakes occurred throughout the entire thickness of the continental crust. Nowhere did they find convincing evidence for *substantial* seismicity in the continental upper mantle, even where the lower crust was seismically active. Furthermore, they observed that the variations in T_s are broadly correlated with variations in T_e, with $T_s \geq T_e$ where T_e was well resolved. They found no example where T_e was required by the data to be larger than T_s, and interpreted their results to indicate that the long-term strength of the continental lithosphere resides in a single seismogenic layer that was either the upper crust or the whole crust, but did not involve the mantle. These observations therefore suggested that the prevalent rheological model of Chen & Molnar (1983), colloquially known as the 'jelly-sandwich' model, required modification, and led to a series of other developments and insights into the nature and causes of lithosphere strength variations, which will be summarized in the later Discussion section.

The views of earthquake depth distribution summarized by Maggi *et al.* (2000a) and Jackson (2002a) have been challenged, with attention focusing on the seismicity of northern India and parts of Tibet. Chen & Yang (2004), Schulte-Pelkum *et al.* (2005) and Monsalve *et al.* (2006) claim that earthquakes do occur in the uppermost mantle in those regions, with a bimodal depth distribution, and that the Chen & Molnar (1983) 'jelly-sandwich' model is still valid. The purpose of this paper is to examine the evidence for the earthquake depth distributions in these regions and also to discuss their causes, contexts and significances for a generic understanding of continental rheology. We will conclude that: (1) there is indeed evidence for microearthquakes, but not substantial seismicity in the uppermost mantle beneath parts of the Himalaya and southern Tibet; (2) this is not in conflict with an understanding of the temperature control of seismicity that has developed since the early papers of Maggi *et al.* (2000a) and Jackson (2002a); (3) that any apparent bimodal depth distribution beneath northern India and the margins of Tibet is a consequence of the particular geological setting of those regions, and does not represent a generic global phenomenon and (4) that the conclusion of Maggi *et al.* (2000a) and Jackson (2002b) that, in general, long-term continental strength resides in either the upper or whole crust, but not substantially in the mantle, is correct.

We pursue these questions with a close scrutiny of the crust and uppermost mantle structure and earthquake depths in peninsula India, the Himalaya and Tibet. We first discuss the variation in Moho depth across northern India, the Himalaya and Tibet and the relationship of the earthquake focal depths to the Moho. We critically examine the cases put forward by Chen & Yang (2004), Schulte-Pelkum *et al.* (2005) and Monsalve *et al.* (2006). After building up a coherent view of the structure and seismicity of the Himalayan collision zone, we assess the significance of the earthquake focal depths for our general understanding of the rheology of the continental lithosphere.

2 MOHO DEPTH AND THE SUB-MOHO MANTLE BENEATH NORTHERN INDIA, THE HIMALAYA AND TIBET

Over the past 20 yr a number of active and passive seismic experiments have provided information on the crust and uppermost mantle velocity structure of Tibet and southern India. However, details of the structure of the Indian Shield as it penetrates the Himalaya and southern Tibet remained sparse until several recent passive seismic experiments across the Himalaya provided the first detailed observations of this region. Active experiments such as seismic reflection and refraction studies provide a detailed description of crustal structure over a limited region, but passive seismic experiments such as receiver functions studies furnish a simple means of examining the gross features of the crust over broad areas, especially in regions where active seismic experiments are difficult or impossible to conduct. Surface wave analyses, especially those incorporating higher modes, provide constraints on the broad-scale seismic structure of the upper mantle. We employ the analysis of receiver functions and surface waves to ascertain the variation in the structure of the seismic lithosphere across the Indo–Eurasian collision zone.

2.1 Crustal structure of the Himalaya and southeast Tibet

Receiver functions are radial waveforms created by deconvolving the vertical component seismogram from the radial component seismogram to isolate the receiver site effect from the other information contained in the teleseismic *P* wave coda. Receiver functions allow the determination of the delay time between the direct *P*-waves (Pp) and the converted *S* waves (Ps) from a velocity discontinuity beneath the station. The Moho is the most common major velocity discontinuity in the lithosphere, and it is the discontinuity of interest in this paper. The Ps–Pp delay time depends on the depth to the Moho and the average velocity of the crust; thus, there is a trade-off, and neither the Moho depth nor the average velocity of the crust can be uniquely determined through receiver-function analysis alone. To minimize the trade-off between Moho depth and average crustal velocity, we simultaneously invert *P*-wave receiver functions and short-period fundamental-mode surface wave dispersion data for the same region. This simultaneous inversion of both data sets provides strong constraints on crustal structure since receiver functions are sensitive to the interface structure but less so to the absolute velocities, whereas the dispersion data are sensitive to the absolute velocities but less so to first-order discontinuities (Julià *et al.* 2000).

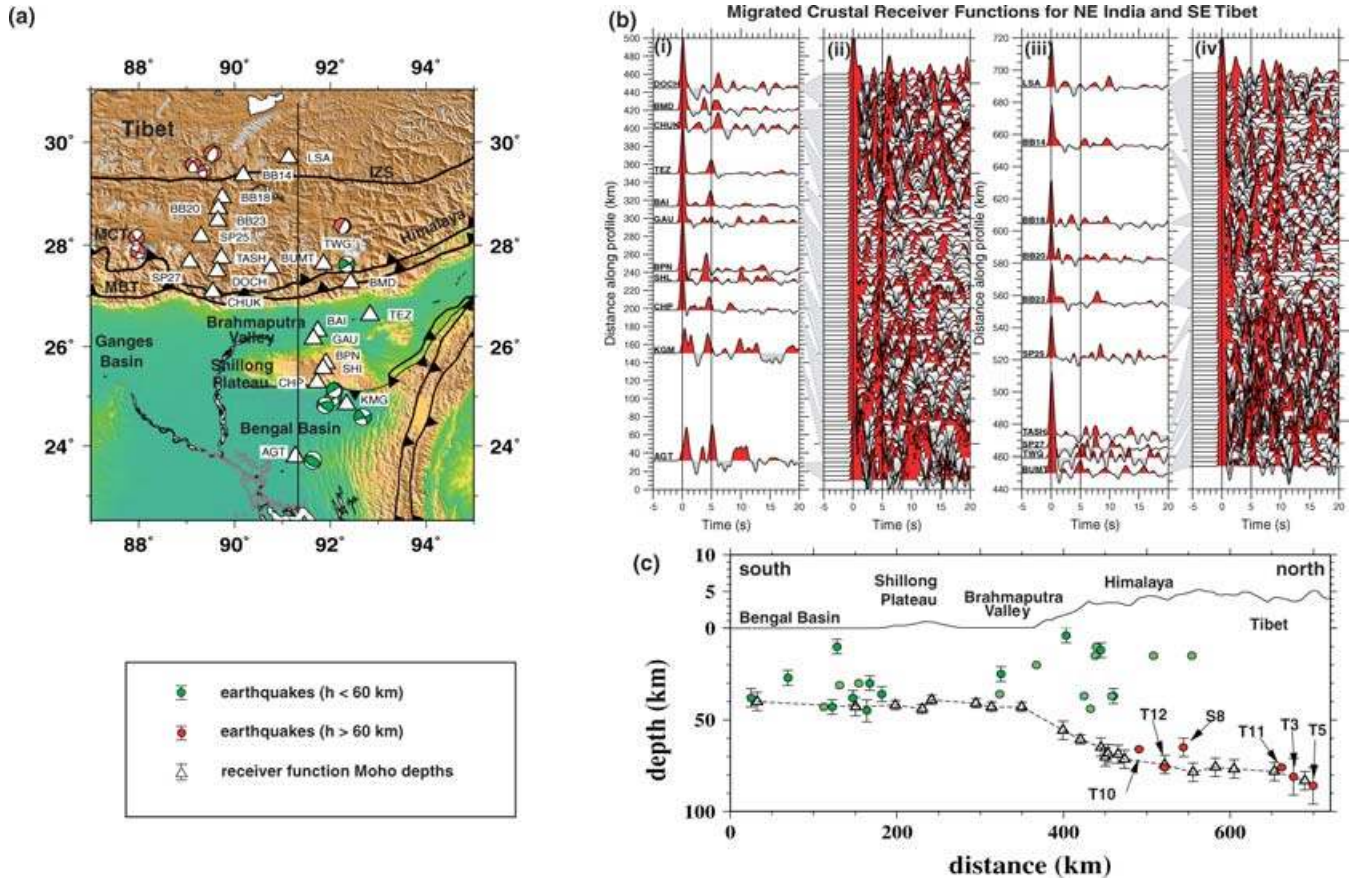

Figure 1. Summary of receiver function analysis and earthquake focal depths for NE India, Bhutan, and SE Tibet. (a) Locations of seismographs (white triangles) providing broad-band seismograms for the profile. (b) Receiver function record at sites indicated and projected on a N–S profile along longitude 91.0°E [black line in (a)]. These receiver functions were computed using the iterative, time-domain deconvolution method (Ligorria & Ammon 1999), the traces are lowpass-filtered with a corner at 0.7 Hz, corrected for distance-moveout of the Moho Ps phase to a reference distance of 67°, and projected onto the N–S profile. The receiver functions from each site are plotted twice; the average receiver function at each site is plotted at the correct projection distance in panels (i) and (iii), and the individual receiver functions are plotted equispaced from south to north in panel (ii) and (iv). This form of plot has the advantage of a constant distance scale in panel (i) and (iii) while also making the phase correlation more clear in panel (ii) and (iv). Panels (iii) and (iv) are the northward extensions of panels (i) and (ii). The Moho Ps phase is noted by the dashed line in panels (ii) and (iv) starting at 4–5 s for the southern receiver functions in panel (ii) and ending at ∼10 s for the northernmost receiver functions in panel (iv). AGT to TEZ and BMD include seismograms used by Mitra *et al.* (2005) and also include more recent seismograms for the same stations; TWG is a new station operated by the Indian Institute of Astrophysics and the University of Cambridge; CHUK, DOCH, BUMT and TASH are PASSCAL stations in Bhutan; SP27 and SP25 to BB14 are INDEPTH II stations (Yuan *et al.* 1997); and LSA is a CDSN station. The Moho Ps phase is clear in the NE India data for TEZ and sites to the south, and in the SE Tibet data for SP25 and sites to the north. For the Himalaya stations (sites CHUK to TASH) the Moho Ps phase can be tracked, but the receiver functions are more complex than receiver functions to the north or south of the Himalaya. (c) Moho depths (open triangles with error bars) determined from simultaneous inversion of the receiver-function data and Rayleigh-wave dispersion data. The location of the profile is indicated by the black line in (a). Earthquakes with well-determined focal depths located ±350 km either side of the profile are projected onto the crustal cross-section (green circles—crustal earthquakes with focal depths <60 km; red circles—deep earthquakes with focal depths >60 km). Earthquake parameters for the lower crustal and deep earthquakes are given in Table 1. Focal depths for all events are determined either by waveform modelling or direct timing of depth phases using the crustal velocity structure determined by the receiver function analysis, giving a focal depth relative to the surface. The zero in (c) is at sea level so the earthquake focal depth and the receiver function Moho depths are the elevation above sea level of the topography plus the depth below sea level plotted in (c). Note the different scales for the elevation and depth in (c).

Mitra *et al.* (2005) used receiver functions to track the Moho of the Indian crust beneath NE India, the Himalaya and SE Tibet. Fig. 1 shows an expanded receiver-function record section of 21 stations along a profile from the Bengal Basin to Lhasa and includes data of Mitra *et al.* (2005) from NE India plus more recently recorded data at the same stations, and data from PASSCAL experiments in Bhutan and SE Tibet (Yuan *et al.* 1997). The results have been projected onto a NS profile nearly perpendicular to the Himalayan front at this longitude (Fig. 1a). Compared with the receiver functions from the south Indian Shield (Rai *et al.* 2003), those from NE India and SE Tibet show much greater complexity. Although the seismographs contributing to this profile lie as much as 200 km off the line, the Moho phase of the receiver function for stations at equivalent positions with respect to the Himalayan front is similar (e.g. CHUC, BMD and DOCH or TEZ and BAI—Fig. 1b).

The southernmost receiver functions from sites AGT and KMG show an apparent delay of the direct *P* wave resulting from the thick sediments of the Bengal Basin (Fig. 1b). Receiver functions from the Shillong Plateau sites SHL, BPN and CHP are relatively simple and broadly similar to receiver functions observed on the south Indian Shield. The delay time of the Ps phase increases from ∼4.5 s for the Shillong Plateau stations to ∼5 s for the Brahmaputra Valley sites

(BAI, GAU, TEZ—Fig. 1b), indicating a slight deepening of the Moho northward due to the downward bending of the crystalline crust as it is thrust beneath the Himalaya and the accumulation of sediment in the Himalayan foredeep. Receiver functions in the Lesser Himalaya (CHUK, BMD and DOCH—Fig. 1b) show two positive arrivals between 3 and 6 s. Mitra *et al.* (2005) considered it unlikely that the earlier phase at BMD was the Moho Ps because this would imply an extremely thin crust beneath the Lesser Himalaya that is inconsistent with gravity observations (Das Gupta & Biswas 2000), and therefore the 6 s phase must be the Moho Ps conversion. The 3.5–4.0 s phase may result from conversion at the decollement surface along which the Indian Plate underthrusts the Himalaya and southern Tibet. The receiver functions become increasingly complex to the north in the Greater Himalaya and SE Tibet. The Ps phase is less definite in the receiver functions of the Greater Himalaya sites (BUMT to TASH—Fig. 1b), but Ps is clear and has a delay of 9-10 s with respect to the direct arrival for receiver functions for the six northern sites (SP25 to LSA—Fig. 1b), indicating a flattening of the Moho. The increasing number of intracrustal arrivals in the Greater Himalayan and SE Tibetan receiver functions towards the north is presumably caused by the internal disruption of the crust which has been shortened.

The earlier study of Mitra *et al.* (2005) inverted the receiver functions without the additional constraints provided by the surface wave data. In this study, Fig. 1(c) shows the variation in Moho depth from NE India to SE Tibet determined by the simultaneous inversion of the receiver function and group velocity data (Mitra *et al.* 2006b). The crust beneath the Bengal Basin and Shillong Plateau is 40–45 km thick. Achaean rocks are exposed on the Shillong Plateau, where the average velocity structure of the crust is similar to that observed beneath the Achaean terrane of the south Indian Shield. There is little change in the Moho depth beneath the Brahmaputra Valley (BAI, GAU and TEZ) and, below the sediments of the Himalayan foredeep, the structure of the crystalline crust appears similar to that found below the Shillong Plateau (SHL, BPN and CHP) (Mitra *et al.* 2005). Beneath the Lesser Himalaya the Moho deepens from ∼58 km below the surface at CHUK to ∼68 km beneath DOCH. Below SE Tibet the Moho deepens further from ∼79 km below the surface elevation of SP25 to ∼87 km depth below LSA (Fig. 1c).

Also plotted in Fig. 1(c) are the positions of earthquakes whose focal depths have been determined using depth phases or waveform fitting. In the south, beneath the Bengal Basin and the Shillong Plateau, earthquakes occur throughout the entire thickness of the crust to the vicinity of the Moho. Beneath SE Tibet earthquakes occur at two levels, most at depths of less than about 20 km in the shallow crust and a few near the base of the crust. The middle level of the Tibetan crust is aseismic. We discuss this earthquake depth distribution in greater detail below.

2.2 Crustal structure of NW India and western Tibet

Rai *et al.* (2006) used teleseismic receiver functions to map the configuration of the Indian Moho along a 700-km profile in NW India and Ladakh extending from Delhi (NDI) on the south side of the Ganges Basin to Taksha (TKS), located on the Karakorum Fault in Ladakh (Fig. 2a). Fig. 2(b) shows a receiver-function record section for these data. NDI, located on a Proterozoic quartzite ridge on the south side of the Ganges Basin, has a weak Moho Ps phase. Receiver functions from KUK, CHD and BDI (Fig. 2b) show an apparent delayed first-arrival and a delayed Ps Moho conversion due to the low-velocity sediments of the Ganges Basin. Like the receiver functions from NE India and SE Tibet, the NW Himalaya and Ladakh receiver functions become progressively more complex from south to north. The Lesser Himalaya receiver functions (BSP to KUL) show a positive arrival at 6–7 s, but, in general, the Moho Ps phase is difficult to trace beneath the Lesser Himalaya. However, KTH and DCH in the high Himalaya give a clear Ps Moho phase at 7–8 s delay time and a relatively simple crust (Fig. 2b). The Moho Ps phase has a nearly constant delay of 8–9 s across Ladakh (sites HNL to TGR).

Results from simultaneous inversion of these receiver function and surface wave dispersion data are shown in Fig. 2(c). The crust beneath NDI is ∼40 km thick, with a relatively transparent structure similar to that of the south Indian Shield (Rai *et al.* 2003). The crust thickens to ∼50 km depth beneath the foothills and to 60–65 km depth below the highest part of the Himalaya. From south of the Indus Zangpo Suture (IZS) to the Karakorum Fault, the Moho deepens from 70 to 75 km below the surface.

Wittlinger *et al.* (2004) used receiver functions to map the Moho north and east of the Karakorum Fault beneath western Tibet, and their Moho depths are included in Fig. 2(c). Their measurements are made along a number of short line segments, two of which are relevant to our discussion; one north of the Karakorum Fault that spans the Bangong Suture (green line in Fig. 2a), and a second spanning the Altyn Tagh Fault (blue lines in Fig. 2a). Their results show that the Moho continues to deepen north of the Karakorum Fault up to the Bangong Suture where the crust is ∼80 km thick. Across the Bangong Suture, there may be a step-like increase of ∼10 km in the Moho depth, and to the north the Moho is relatively flat at ∼90 km depth below the surface. In the vicinity of the Altyn Tagh Fault the Moho shallows to 50–60 km depth, and then to ∼50 km beneath the Tarim Basin.

Also plotted in Fig. 2(c) are the positions of moderate-sized earthquakes whose focal depths are determined by depth phases or waveform modelling. As beneath SE Tibet, the shallow crust beneath NW Tibet is seismically active, the mid-crust is aseismic, and a few moderate-size earthquakes occur very near the Moho. We return to this in the next section.

2.3 The Moho beneath the central Himalaya and southcentral Tibet

Schulte-Pelkum *et al.* (2005) stacked receiver functions to image the topography of the Indian Moho as it descends beneath the Himalaya in eastern Nepal (near 86°E), but without inverting the data for the velocity structure. They find that in this region, too, the Indian Moho is offset smoothly downward from ∼45 km depth in southern Nepal to ∼75 km depth below sea level (∼80 km below the surface) in southcentral Tibet. Their results, though lacking the velocity and depth control from simultaneous inversion of receiver functions and surface wave dispersion, are similar to those in Figs 1 and 2. Thus, across the whole Himalayan belt, the Indian crust appears to thicken gradually from ∼40 km at the southern edge of the Himalayan foredeep, to 60–65 km beneath the High Himalaya and to 75–90 km beneath western and southern Tibet.

2.4 Upper-mantle seismic structure

The nature of the sub-Moho mantle is also important to our discussion. The sub-Moho seismic structure is most commonly determined by surface waves, and there have been a number of surface wave studies of India (Bhattacharya 1974, 1981; Hwang & Mitchell

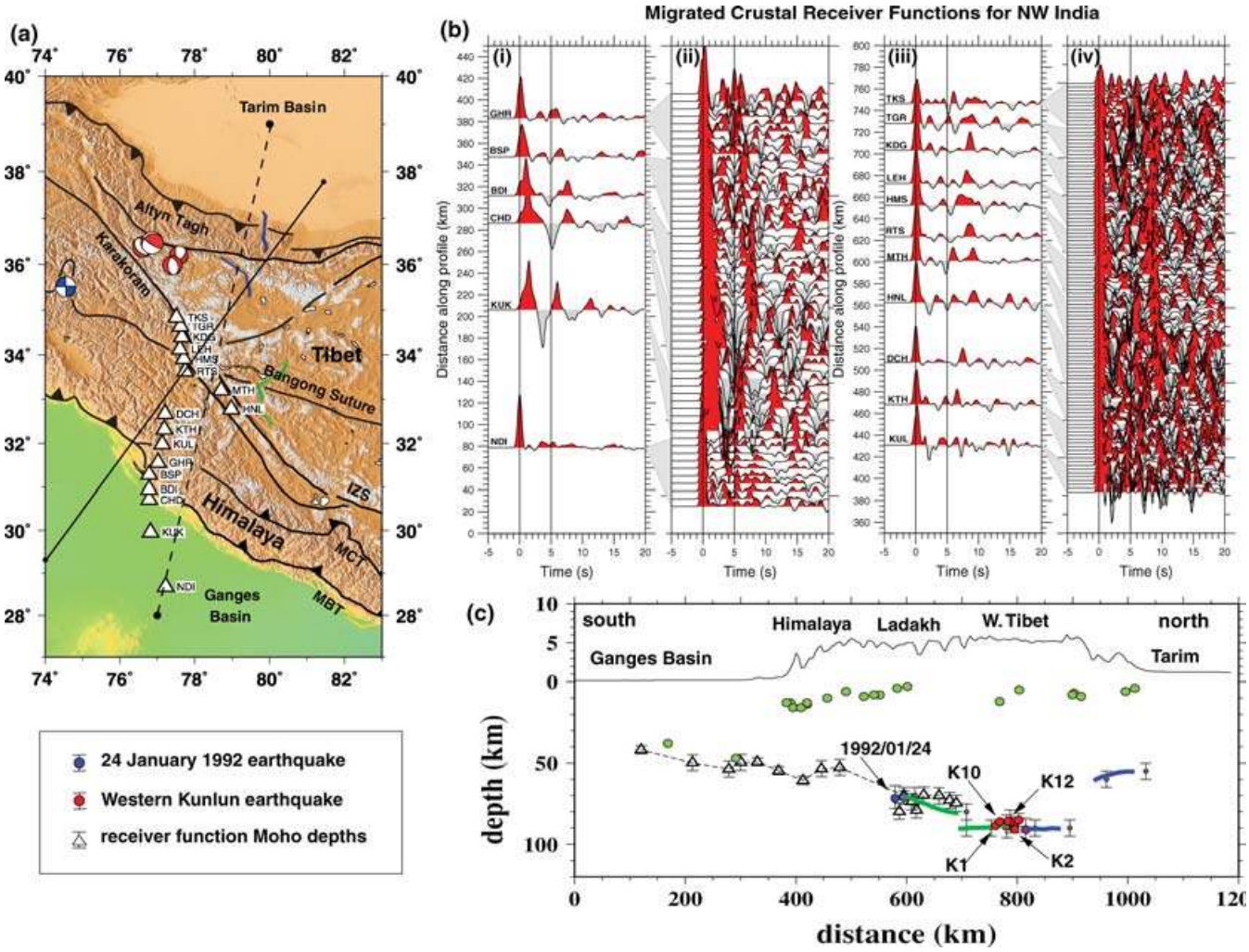

Figure 2. Summary of receiver function analysis and earthquake focal depths for NW India, Ladakh and western Tibet. (a) Locations of seismographs (white triangles) providing broad-band seismograms for the NW India–Ladakh profile and the receiver function profiles of Wittlinger *et al.* (2004) (short blue and green lines). The profile of stations is not laid out perpendicular to the Himalayan front because of the limited access in this part of the Himalaya and Ladakh. (b) Receiver function record at sites indicated by white triangles in (a) projected on a NNE–SSW profile with endpoints 28°N, 77°E and 39°N, 80°E [black dashed line in (a)]. The Moho Ps phase is denoted by dashed line in panels (ii) and (iv) starting at 4–5 s for the southern receiver functions in panel (ii) and ending at ∼9 s for the northernmost receiver functions in panel (iv). Ps is clear in the data for the Ganges Plain and the Lesser Himalaya (GHR and sites to the south), but the receiver functions become much more complex for sites in the Greater Himalaya (KUL—DCH) and Ladakh (HNL—TKS). (c) Moho depths (open triangles with error bars) determined from simultaneous inversion of the receiver function and Rayleigh wave dispersion data in northern India, the Himalaya and Ladakh (Rai *et al.* 2006), and Moho depths in NW Tibet from migrated receiver functions (Wittlinger *et al.* 2004) projected on a profile with endpoints 29.4°N, 74°E and 38°N, 81.5°E [black line in (a)]. This line is perpendicular to the Himalayan front at this longitude but oblique to the receiver function profile. Earthquakes with well-determined focal depths located ±350 km either side of the profile are projected onto the crustal cross-section (green—crustal earthquakes <60 km, red—deep events in the western Kunlun, blue—deep earthquakes in the Himalaya, Table 1). Focal depths for all events are determined either by waveform modelling or direct timing of depth phases using the crustal velocity structure determined in the receiver function analysis. Format for this figure is the same as for Fig. 1.

1987; Mitra *et al.* 2006b) and Tibet (Romanowicz 1982; Brandon & Romanowicz 1986; Bourjot & Romanowicz 1992; Griot *et al.* 1998; Curtis *et al.* 1998; Ritzwoller & Levshin 1998), the majority of which rely on fundamental-mode observations. Fig. 3 is the upper mantle S_v-model of Priestley *et al.* (2006) for the Asian upper mantle derived from the analysis of a large, multi-mode Rayleigh-wave data set. Including higher-mode surface waves is important for resolving the upper-mantle structure beneath India and Tibet. Details of the derivation and resolution test of this model are given by Priestley *et al.* (2006).

At 125 km depth (Fig. 3a) the south Indian Shield is fast with respect to the modified PREM (Dziewonski & Anderson 1981) reference model (Fig. 3d), but by 175 km depth (Fig. 3b), beneath the shield wave speeds are similar to that of the reference model. Fig. 3(c) shows a profile through the model extending across India, the Himalaya and Tibet. Fast mantle underlies southern India to ∼160 km depth but thickens significantly beneath northern India. From long-period Rayleigh-wave phase-velocity measurements made within southern India, Mitra *et al.* (2006a) found that the high-velocity lid beneath the region had an average thickness of about 155 km, in agreement with the tomographic model shown in Fig. 3. Southern Tibet is fast at 125 km depth, but a large region of northern Tibet is slow with respect to the reference model (Fig. 3a). However, at 175 km depth (Fig. 3b) the mantle beneath all of Tibet is fast.

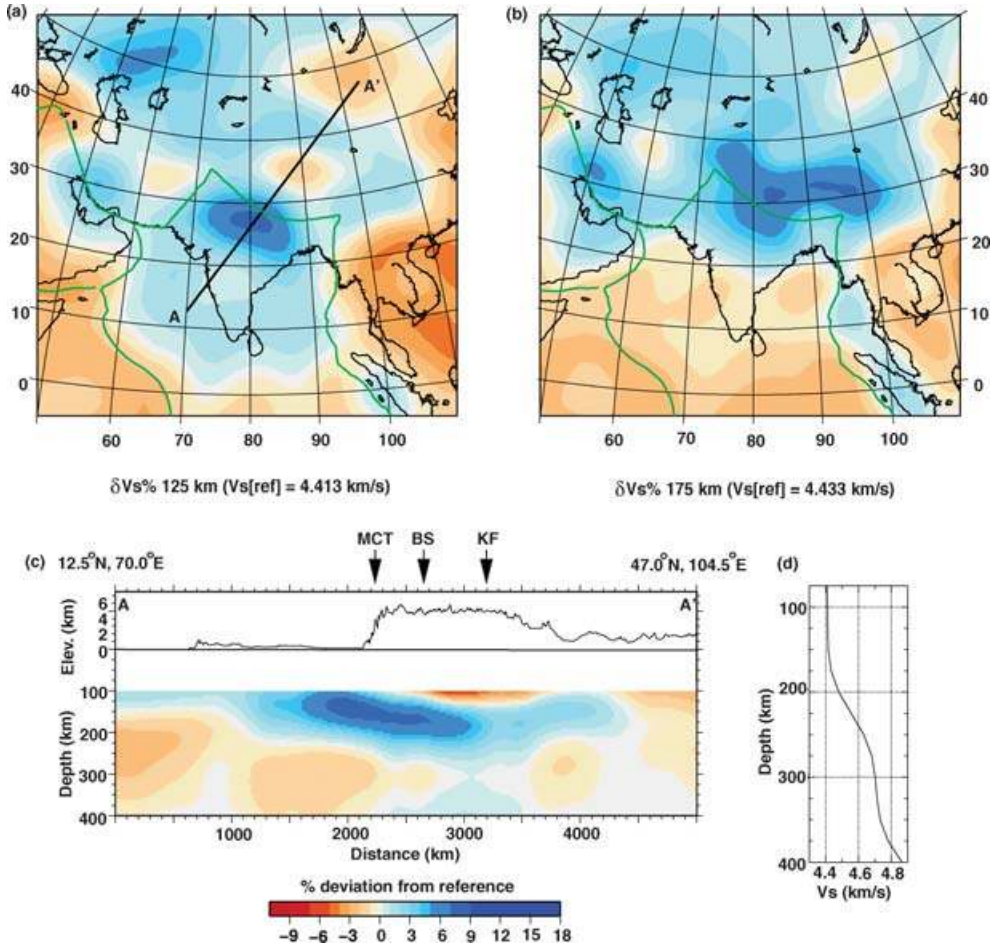

Figure 3. Depth sections through the surface wave tomography model are shown at (a) 125 km and (b) 175 km depth. Each of the depth sections has the reference model velocity (Vsref) at the depth indicated beneath the map. Green lines denote tectonic features. (c) Profiles show the topography and depth variation of the S_V-wave speed heterogeneity with the position of the Main Central Thrust (MCT), the Bangong Suture (BS) and Kunlun Fault (KF) indicated. The location of the endpoints of the profile is shown in (a). Because of the extreme thickness of the Tibetan crust, only mantle results below 100 km depth are plotted. (d) Reference model. The percentage deviation from the reference velocity in (a), (b) and (c) is denoted by the scale below the profile shown in (c).

Fig. 3(c) shows fast mantle dipping northward beneath northern India and the Himalaya and reaches ∼250 km depth beneath southern and central Tibet. North of Tibet the high velocity upper-mantle lid extends to 175–200 km depth but dips to the south beneath northern Tibet.

At the resolution of the Priestley *et al.* (2006) surface wave model, the whole of Tibet is underlain by high-wave speed upper-mantle material to a depth of 225–250 km. McKenzie & Priestley (2007) suggest that the thin low-velocity, sub-Moho layer beneath northern Tibet is likely due to a temperature inversion caused by radioactive heating in the thickened Tibetan crust. The upper-mantle model in Fig. 3 is consistent with the underthrusting of Indian lithosphere from the south and Asian lithosphere from the north (e.g. Matte *et al.* 1997; Tapponnier *et al.* 2001) or with the near-horizontal underthrusting of Indian lithosphere beneath all of Tibet (e.g. Ni & Barazangi 1983; Zhou & Murphy 2005). Because of the smoothing due to the long wavelengths of the surface wave data, we cannot rule out a narrow upwelling beneath the plateau as proposed by Tilmann *et al.* (2003). However, Fig. 3 is inconsistent with the wholesale delamination of the high velocity lid beneath Tibet and its replacement by hot asthenospheric mantle (e.g. Houseman *et al.* 1981; England & Houseman 1989). The importance of the India–Tibet surface wave model to this study is that the lower Indian crust underlying southern Tibet is insulated from the hot asthenosphere by a thick layer of cool lithospheric mantle (Fig. 3).

3 INDIAN, HIMALAYAN AND SOUTH TIBETAN SEISMICITY

The Indian Shield south of the Himalayan front has a low but significant level of seismicity (Fig. 4). Earthquakes in south India with well-constrained focal depths determined by waveform modelling, direct timing of depth phases or local network recording occur within the crust, mainly at shallow depths (<15 km). However, focal depths determined by waveform modelling of 35 km for the 1997 May 21 M_w 5.7 Jabalpur earthquake in central India (Maggi *et al.* 2000b; Rao *et al.* 2001), of 20 km for the 2001 September 5 M_w 4.8 earthquake along the south Indian coast (11°N, 80°E—Fig. 6) (Jackson, unpublished results), of ∼40 km for several earthquakes in the vicinity of the Shillong Plateau (Mitra *et al.* 2005) and Rajasthan (Jackson 2002b), as well as studies of the 2001 Bhuj aftershocks using data from a dense local seismic network (Bodin & Horton 2004), demonstrate that the whole thickness of the Indian crust is seismically active, at least in some places, and that the Indian crust appears to form a single seismogenic layer. Numerous studies reveal that

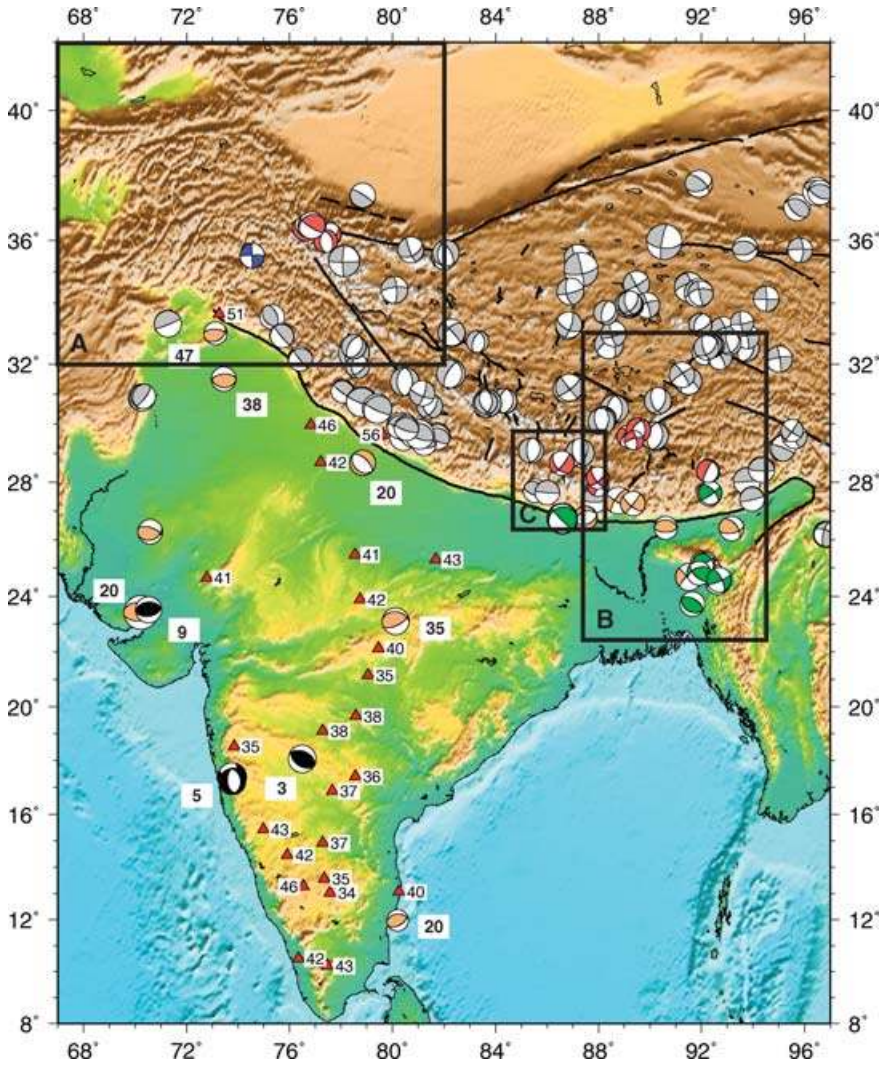

Figure 4. Focal mechanisms of earthquakes in India, the Himalaya and Tibet: shallow crustal events in India (black, depth, $d < 20$ km), mid- to lower-crustal events in India (orange, $20 < d < 35$ km), deep crustal events in NE India (green, $35 < d < 60$ km) and deep events beneath the Himalaya and Tibet (red and blue, 60 km $< d$). All of these events have focal depths constrained by waveform modelling or direct timing of depth phases and their focal depths are calculated using the velocity structure determined from the receiver function analysis. Grey focal mechanisms are for earthquakes from the Harvard CMT catalogue and are likely to be shallower than 15 km. Bold numbers in white boxes near focal mechanisms for earthquakes in the Indian Shield denote focal depths; small numbers in white boxes give Moho depths determined by receiver function analysis at various points in India (Priestley, unpublished results; Gupta *et al.* 2003; Rai *et al.* 2003). The two areas outlined by the black rectangles (A and B) are shown in more detail in Figs 5 and 6. The black rectangles denoted by C denotes the area of the Monsalve *et al.* (2006) study.

unusually deep (70–90 km) earthquakes occur beneath the Himalaya and southern Tibet (Chen & Molnar 1983; Chen 1988; Chen & Molnar 1990; Kayal *et al.* 1993; Chen & Kao 1996; Monsalve *et al.* 2006), principally in two regions; beneath the western Himalayan syntaxis and the western Kunlun Mountains, and beneath SE Tibet and NE India. These unusually deep continental earthquakes have become the centre of controversy of the rheological models for the continental lithosphere.

3.1 The western Himalayan syntaxes and the western Kunlun Mountains

The deep seismicity of the western Himalayan syntaxis and western Kunlun Mountains is shown in Fig. 5(a). Chen & Yang (2004) discuss eight deep earthquakes in this region (denoted by the red focal spheres in Fig. 5(a), also see Table 1) which they claim are in the mantle; also plotted in Fig. 5(a) are other well-located earthquakes in this region from the EHB catalogue (Engdahl *et al.* 1998) and one event (blue focal sphere) whose focal depth is 71 km (Jackson, unpublished results). Chen & Yang (2004) claim that the event labelled H8 in the western Himalayan syntaxis occurred '. . . 150 km southward from the dense zone of earthquakes associated with remnant subduction zone(s) near the Hindu Kush', and therefore is not part of the Hindu Kush seismicity. As the inset in Fig. 5(a) shows, event H8 does indeed lie ∼150 km south of the *deepest* events at 250 km or more beneath the Hindu Kush. The nature of this event is inconclusive, but it seems to us that it is probably associated with the shallower southern portion of the Hindu Kush deep seismic zone.

The other seven events discussed by Chen & Yang (2004) occurred beneath the western Kunlun Mountains (Fig. 5a and Table 1). A western group of three of these earthquakes (K4, K11 and K13

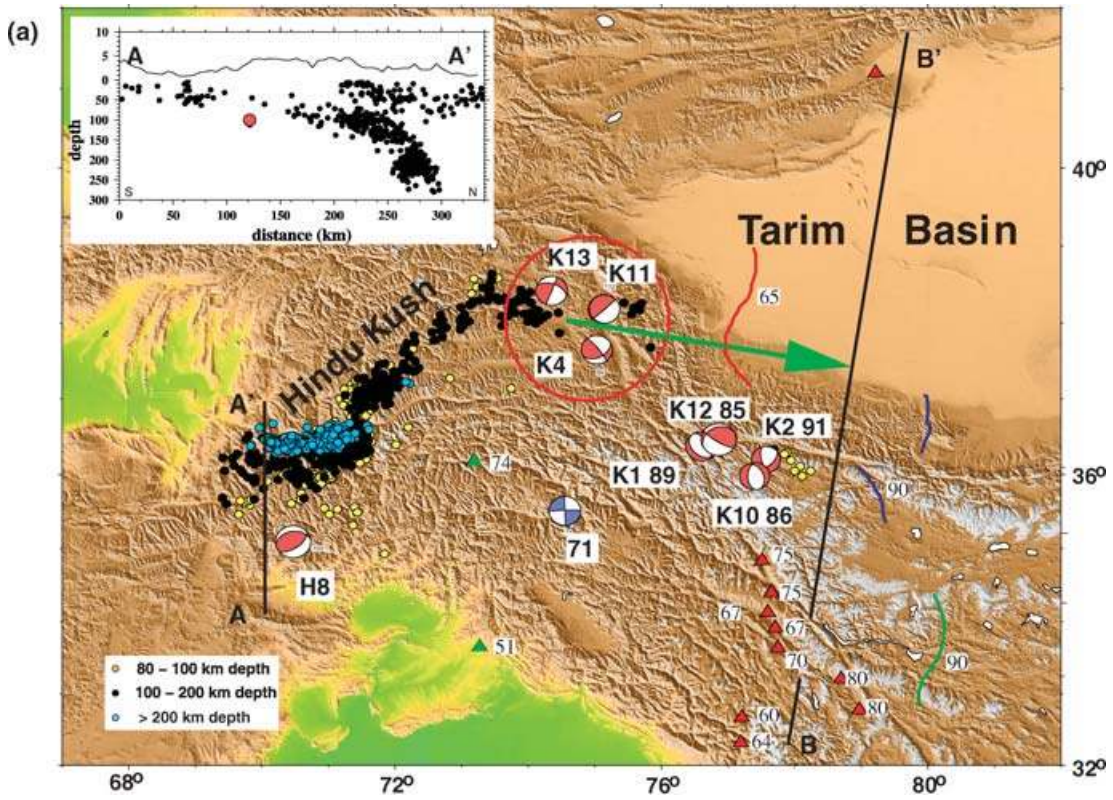

Figure 5. Relationship between earthquake focal depths and crustal structure beneath western Tibet. (a) Topographic map of western Tibet. Red fault-plane solutions are deep events from Chen & Yang (2004); the blue fault-plane solution is from Jackson (unpublished result). Events K4, K11, K13, and possibly H8 are part of the Hindu Kush deep seismic zone. Events K1, K2, K10 and K12 are annotated with their focal depth from this study in km (bold font in white squares). Seismicity denoted by the black, gold and blue dots are from the EHB earthquake catalogue (Engdahl *et al.* 1998) and the depth legend for these events is shown in the lower left corner of the map. Red triangles denote locations of seismograph sites with receiver function crustal thickness (small numbers in white squares) from Rai *et al.* (2006), green triangles denote seismic stations NIL and DBM2 annotated with crustal thickness in km from simultaneous inversion of receiver functions and group velocity data (Priestley, unpublished results). Short red, blue and green line segments denote locations of the receiver function profiles of Wittlinger *et al.* (2004) with receiver-function Moho depths also denoted in km. Both Moho depths and earthquake focal depths are referred to the surface. Line A–A′ and B–B′ shows locations of the cross-sections. The inset in the upper left of (a) is the cross-section along profile A–A′ showing earthquake depths in the Hindu Kush seismic zone from the EHB earthquake catalogue. The red dot denotes the location of event H8 (Table 1). Earthquakes ±100 km from the profile denoted by the line A–A′ on the map are projected onto the profile cross-section in the inset. The shallow events in the southern part of the Hindu Kush zone shown in the inset are left off the map for clarity. (b) Chen & Yang (2004)'s adaptation and modification (their Fig. 1E) of the receiver function results of Wittlinger *et al.* (2004) with earthquake mechanisms superimposed at Chen and Yang's focal depths. The large green arrow in (a) shows where Chen & Yang (2004) project the hypocentres of events K4, K11 and K13 onto the receiver-function profile of Wittlinger *et al.* (2004). (c) Original receiver function results from Wittlinger *et al.* (2004) (their Fig. 4) from which Chen & Yang (2004) extracted the profile shown in (b). Energy denoted in red results from an increase of velocity with depth; energy denoted in blue results from a decrease of velocity with depth. Wittlinger *et al.* (2004)'s interpretation of the Moho is denoted by the dashed line in (b) and (c); Chen & Yang (2004)'s Moho based on the assumption of Airy isostasy is denoted by the doted line in (b). Wittlinger *et al.* (2004)'s Moho corresponds to a velocity increase with depth; Chen & Yang (2004)'s Moho corresponds to a velocity increase with depth over most of the profile but corresponds to a velocity decrease with depth at A in (b), disguised in the grey-tone plotting. A line at 100 km depth has been added for reference to both cross-sections. The seismic arrivals at B and C in (c) occur at greater than 100 km depth in Wittlinger *et al.* (2004)'s profile but in (b) are plotted at less than 100 km depth in Chen & Yang (2004)'s adaptation of Wittlinger *et al.* (2004)'s profile. In (c) KF—Karakorum Fault, SS—Shiquanhe Suture, BS—Bangong Suture, GF—Gozha Fault, ATF—Altyn Tagh Fault, KS—Kudi Suture (all taken from Wittlinger *et al.* (2004). Chen & Yang (2004) project events K4, K11 and K13 onto the crustal profile 75–125 km north of the Moho offset that Wittlinger *et al.* (2004) associate with the Altyn Tagh Fault.

within the red circle in Fig. 5a) at depths of 90–110 km are, according to Chen & Yang (2004) 'unrelated to remnants of subduction in the Hindu Kush'. Chen & Yang (2004) do not show the other seismicity of the Hindu Kush in their paper; we do in Fig. 5(a). These three events are clearly at the eastern end of the contorted Hindu Kush slab (see also Pegler & Das 1998). In order to illustrate the relationship of these three events to the Moho, Chen & Yang (2004) then project the focal depths of events K4, K11 and K13 ∼400 km eastwards onto the receiver-function crustal cross-section of Wittlinger *et al.* (2004) (nearly parallel to the seismometer profile shown as a dashed line in Fig. 2a). The green arrow in Fig. 5(a) shows how Chen & Yang (2004)'s projection places these earthquakes in a completely misleading position on their cross-section (Fig. 5b). Since the Kunlun Mountains form an arc concave to the NE, these earthquakes are given the appearance of occurring beneath the Tarim Basin or northern margin of the Kunlun, where Wittlinger *et al.* (2004) show the Moho is 50–60 km deep (red circle in Fig. 5b). Aside from the strong likelihood that these three earthquakes are part of the Hindu Kush deep seismic zone anyway, Chen & Yang (2004)'s projection of them places them completely out of their geological context. To use these three earthquakes to argue for seismogenic mantle beneath the Tarim and Kunlun margin is disingenuous and simply wrong.

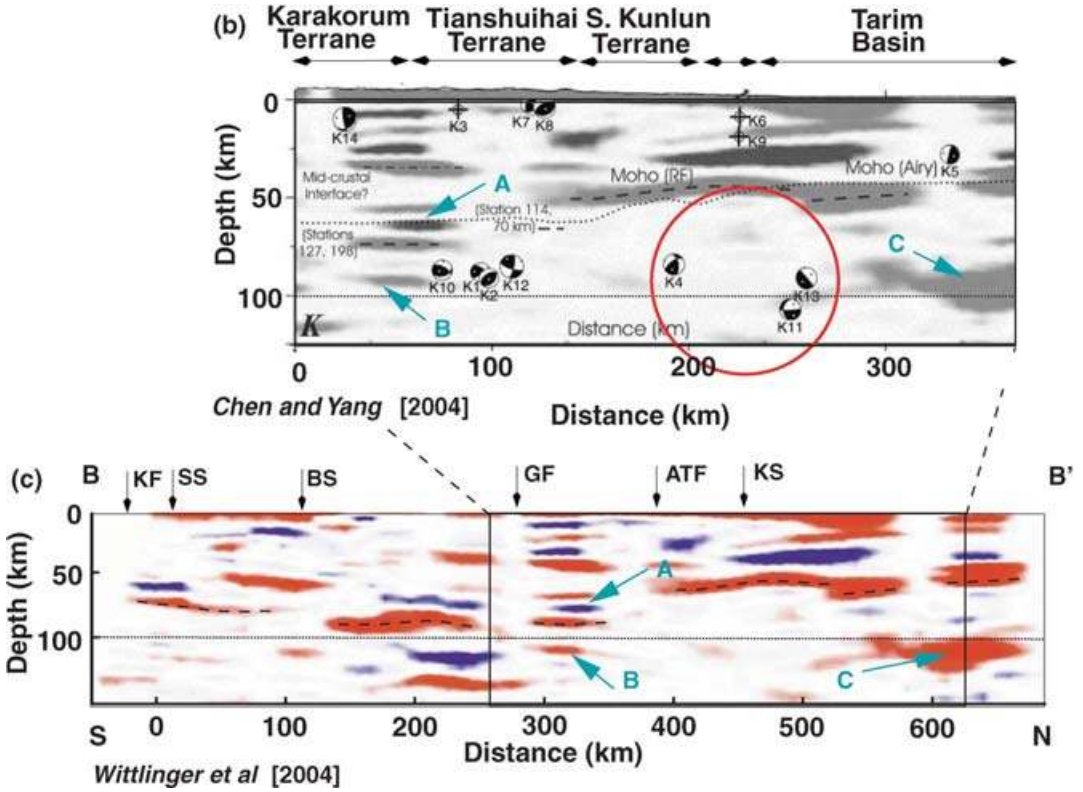

Figure 5. (*Continued.*)

More interesting is an eastern group of four earthquakes—K1, K2, K10 and K12—at 80–90 km depth, which occurred closer to Wittlinger *et al.* (2004)'s profiles. Chen & Yang (2004) reproduced a black-and-white extract from the colour cross-section published by Wittlinger *et al.* (2004), given again here in Fig. 5(b), on which they show these four earthquakes, apparently well below the Moho. This is, at first appearance odd, since Wittlinger *et al.* (2004) claimed that the Moho was at about 90 km. Several features of Fig. 5(b) need clarification. First, Chen & Yang (2004) changed the depth scale on Wittlinger *et al.* (2004)'s profile, which is shown in its original colour form in Fig. 5(c). This change can be seen by comparing the dotted line at 100 km and the features we have marked with arrows A, B and C on both figures. Their justification for doing this was that Wittlinger *et al.* (2004) did not have accurate absolute crustal velocities, just receiver functions, and Chen & Yang (2004) were adjusting the Wittlinger *et al.* (2004) depth scale to be consistent with the crustal velocities ($V_p = 6.0$ km s^{-1} and $V_s = 3.46$ km s^{-1}) they used in calculating the earthquake focal depths. However, the Wittlinger *et al.* (2004) velocity model is consistent with the results of Rai *et al.* (2006) which are determined by simultaneous inversion of receiver function and surface wave dispersion data. The Moho identified by Wittlinger *et al.* (2004) is shown by the dashed lines in both the black-and-white and colour figures. Chen & Yang (2004) chose to identify their own Moho, based on an assumption of Airy isostasy, which is shown by a dotted line in Fig. 5(b). Aside from whether the assumption of Airy isostasy beneath the margin of a foreland basin is a reasonable assumption or not, and the unknown densities at depth, Chen & Yang (2004)'s Moho goes through a *negative* (i.e. blue) reflection coefficient contrast on Wittlinger *et al.* (2004)'s profile, marked A by the green arrows in Figs 5(b) and (c), thus requiring a mantle velocity lower than that in the crust. Finally, Chen & Yang (2004) fail to make clear that these four earthquakes lie south of the Altyn Tagh Fault across which Wittlinger *et al.* (2004) detected a big step in the Moho, to a depth of 90 km in the south. As is clear from Fig. 5(c), *all* of Wittlinger *et al.* (2004)'s Moho estimates south of the Altyn Tagh Fault are in the range 85–90 km. In our opinion, seismic constraints on the Moho depth are more robust than values based on gravity or assumptions of Airy isostasy, and it makes little sense to adjust the well-constrained crustal thickness from seismology to agree with a more poorly constrained value based on gravity or topography. Chen & Yang (2004)'s events K1, K2, K10 and K12 occur south of the Altyn Tagh Fault at 90–96 km depth, well below their gravity-constrained Moho which lies between 63 and 67 km depth (Fig. 5c) but close to the seismically constrained Moho at 90 $\pm$ 4 km (Wittlinger *et al.* 2004).

The blue focal mechanism on Fig. 5(a) denotes the 24 January 1992 event which occurred at 71 $\pm$ 4 km depth. The Moho depth at station DMB2 (green triangle), 140 km along-strike of the range to the NW, is 74 $\pm$ 4 km, and is essentially the same as the Moho depth beneath stations in the same relative position to the SE on the Rai *et al.* (2006) profile (red triangles), suggesting that this earthquake also occurred very near the Moho, possibly in the lower crust.

In Fig. 2(c), we have replotted the focal depths of events K1, K2, K10 and K12 (in red) and the focal depth of the 24 January 1992 event (in blue) relative to the Moho of the crustal model of Rai *et al.* (2006) and Wittlinger *et al.* (2004). The five events occur close to the seismologically determined Moho. The focal depths for these earthquakes shown in Fig. 2(c) and listed in Table 1 are based on identification of surface reflections (pP–P or sP–P times), and were calculated using the crustal velocity structure determined by the receiver-function and surface wave analysis. Thus, both the Moho depth beneath the seismograph site and the focal depth of

Table 1. Summary of source parameters of deep earthquakes in the western syntaxis, western Tibet, southeastern Tibet and northeast India whose depths are constrained by waveform analysis.

ID	Date	Time	°N	°E	Dep*	mb	Fault plane	Dep†	Dep‡	Location	Source
H8	1990/10/25	04:54	35.091	70.476	112	6.0	260 34 113	100 ± 08		Hindu Kush	Chen & Yang (2004)
K1	1963/06/26		36.38	76.61			133 38 −105	93 ± 07	89	Western Kunlun	Chen & Yang (2004)
K2	1965/06/22	05:49	36.198	77.571	101	4.9	164 64 −134	96 ± 07	91	Western Kunlun	Chen & Yang (2004)
K4	1972/01/12	18:37	37.648	75.035	100	5.3	322 81 133	89 ± 07		Hindu Kush	Chen & Yang (2004)
K10	1976/10/01	11:27	35.982	77.404	89	5.1	336 41 −109	92 ± 07	86	Western Kunlun	Chen & Yang (2004)
K11	1977/07/29	09:14	38.187	75.144	125	5.3	158 5 21	112 ± 10		Hindu Kush	Chen & Yang (2004)
K12	1980/02/13	22:09	36.473	76.856	95	6.0	122 78 112	90 ± 04	85	Western Kunlun	Fan & Ni (1989), Chen (1988)
K13	1990/05/17	13:21	38.423	74.356	107	5.5	290 50 179	96 ± 07		Hindu Kush	Chen & Yang (2004)
	1992/01/24	05:04	35.506	74.551	71				71	Western Himalayan	This study
T3	1973/08/01	14:05	29.566	89.141	93	4.9	220 60 −24	85 ± 10	81	Himalaya and S. Tibet	Molnar & Chen (1983)
T5	1976/09/14	06:43	29.782	89.544	102	5.4	215 52 −68	90 ± 10	86	Himalaya and S. Tibet	Chen *et al.* (1981)
T8	1986/01/10	03:46	28.654	86.567	79	5.5	140 46 −163	85 ± 10	81	Himalaya and S. Tibet	Ekström (1987), Chen (1988)
T9	1988/08/20	23:09	26.731	86.591	57	6.4	246 20 22	51 ± 05		Himalaya and S. Tibet	Chen & Kao (1996)
T10	1991/12/21	19:52	27.878	87.984	45	4.7	112 82 −179	70	66	Himalaya and S. Tibet	Zhu & Helmberger (1996)
T11	1992/03/07		24.99	89.37		4.3	350 68 −164	80	76	Himalaya and S. Tibet	Zhu & Helmberger (1996)
T12	1992/04/04	17:43	28.151	87.958	49	4.9	46 66 −22	80	76	Himalaya and S. Tibet	Zhu & Helmberger (1996)
S1	1963/06/19		24.97	92.06			57 80 42	52 ± 06	45	Shillong Plateau	Chen & Molnar (1990)
S2	1963/06/21		25.13	92.09			238 88 −70	38 ± 04	36	Shillong Plateau	Chen & Molnar (1990)
S4	1968/06/12	04:29	24.820	91.894	43	5.3	132 60 135	41 ± 04	38	Shillong Plateau	Chen & Molnar (1990)
	1971/02/02	07:59	23.720	91.639	45	5.4	119 36 90	46 ± 05	38	Shillong Plateau	Chen & Molnar (1990)
S8	1996/06/09	23:25	28.383	92.252	78	5.1	206 79 −79	69 ± 05	65		Chen & Yang (2004)
	1995/02/17	02:44	27.626	92.342	37	5.1	317 62 167		37	Shillong Plateau	Mitra *et al.* (2005)
	1996/11/19	00:12	24.589	92.677	48	5.4	67 79 17		43	Shillong Plateau	Mitra *et al.* (2005)
	1997/05/08	02:53	24.906	92.231	33	5.6	239 79 2		30	Shillong Plateau	Mitra *et al.* (2005)
	2000/09/05	00:32	17.257	73.808	10	5.4	351 39 −94		06	South India	This study
	2001/09/25	14:56	11.965	80.198	24	4.8	265 40 109		20	South India	This study

Notes: The event ID is taken from Chen & Yang (2004), the event origin time and epicentre from the EHB catalogue when available and from Chen & Yang (2004) for events prior to 1964. Three focal depths in kilometres are given for each event: the focal depths from the catalogue of Engdahl *et al.* (1998) or its updated web version (*); focal depths from cited references (†) and focal depths based on the crustal velocity model of this study (‡).

the earthquake are based on a crustal delay time below the surface and using the same crustal velocity model. Any bias in the crustal thickness and the earthquake focal depths will therefore be similar. The absolute errors in both the crustal thickness and the earthquake focal depths are probably about ±4–5 km. Although Chen & Yang (2004) use very low average velocities for the crust ($V_p = 6.0\,\mathrm{km\,s^{-1}}$ and $V_s = 3.46\,\mathrm{km\,s^{-1}}$), they do not state what mantle velocities they have used in determining the earthquake focal depths they claim are in the mantle. The data in the supplement to Chen & Yang (2004) suggest they used a P_n velocity of 8.3–8.4 $\mathrm{km\,s^{-1}}$, significantly higher than has been reported for Tibet (e.g. McNamara *et al.* 1997).

In conclusion, and ignoring the deep seismic zone of the Hindu Kush, it is clear that the five earthquakes plotted on the cross-section of Fig. 2(c) occurred very close to the Moho beneath NW Tibet. Given the errors in both Moho and focal depth determinations, we cannot say unequivocally that they were in either the upper mantle or the lower crust. As we show next, a similar case can be made for earthquakes in a part of SE Tibet, and in Section 4, we investigate what their significance might be.

3.2 SE Tibet and NE India

In SE Tibet, earthquakes occur in the upper crust to ∼20 km depth, the mid-crust is aseismic, and a few deep earthquakes occur at 70–90 km depth (Fig. 6). Chen & Yang (2004) argue that these unusually deep continental earthquakes beneath SE Tibet are too deep to have occurred in the crust and that they must have also taken place in the upper mantle. A few earthquakes occur at ∼40–45 km depth beneath NE India, and Chen & Yang (2004) suggest that these earthquakes may also occur below the Moho.

Fig. 6 compares the focal depths of the deep events in SE Tibet and NE India with the nearby crustal thickness determined by receiver function analysis. The earthquake focal depths and crustal thickness values are calculated using the same crustal velocity model derived from the simultaneous inversion of receiver-function and surface wave-dispersion data, and earthquake focal depths are projected onto the crustal cross-section in Fig. 1(c). Beneath SE Tibet, the deepest events occur at 75–90 km depth in a region where the seismologically determined Moho is 75–90 km deep. Mitra *et al.* (2005) found that beneath NE India in the region of the Shillong Plateau, the entire thickness of the crust was seismically active, and the deepest events occurred at ∼40 km depth, very near the seismologically determined Moho.

As with the western Kunlun, we conclude that the deepest earthquakes shown in Figs 1(c) and 6 occurred very close to the Moho beneath both Shillong and SE Tibet. Again, allowing for errors, a balanced judgement would conclude that it is not possible to say for certain whether they occurred in the lower crust or uppermost mantle. However, we do know with certainty that the lower crust of India is seismically active south of the range front (Fig. 1c).

3.3 Microearthquakes beneath the eastern Himalaya

Several studies have used data from seismic networks in the Himalaya to locate earthquakes beneath eastern Nepal, NE India, and southernmost Tibet (Kayal *et al.* 1993; Kayal 2001; Langin

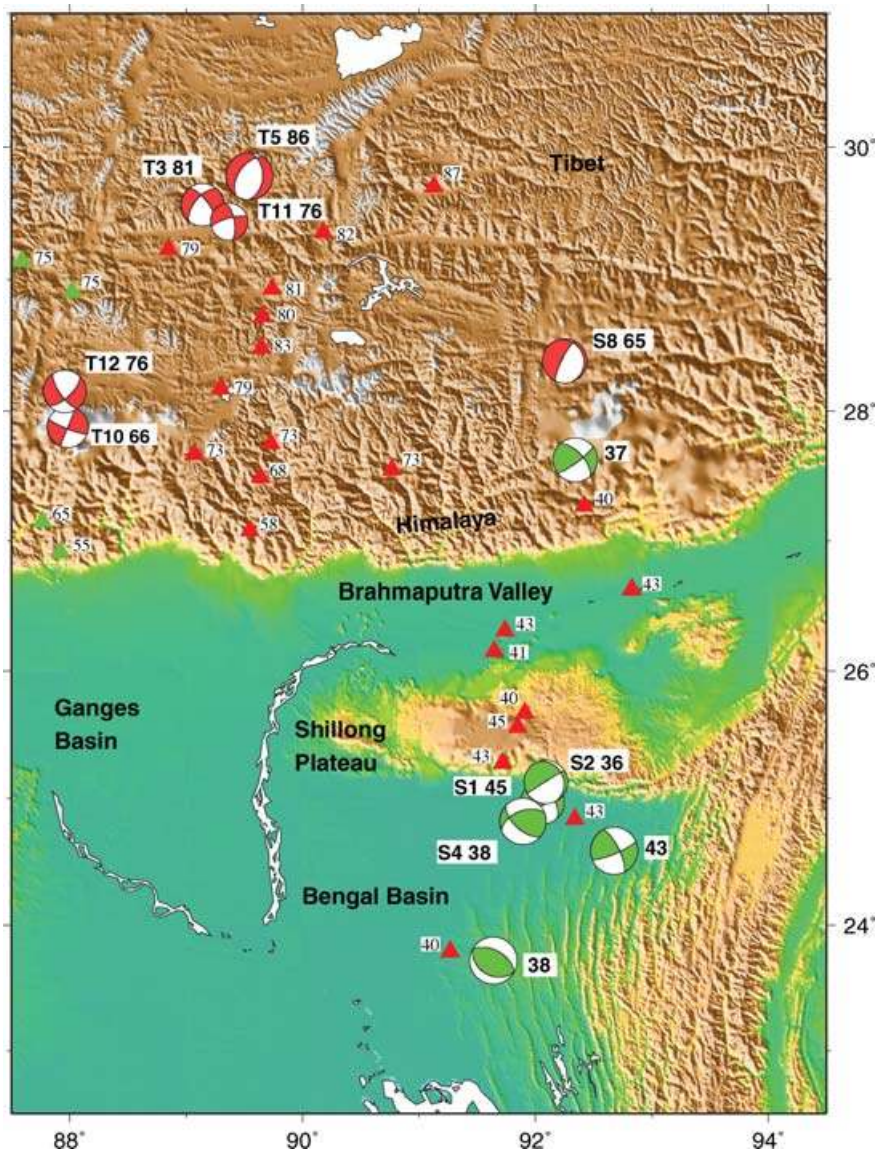

Figure 6. Relationship between earthquake focal depths and crustal structure beneath NE India and SE Tibet. Green (35–60 km deep) and red (>60 km deep) focal mechanisms denote events with well-constrained focal depths. Event designation from Table 1 and focal depth (in bold) are given next to each focal sphere. Red triangles denote locations of seismograph sites annotated with the Moho depth (in km) from Fig. 1(c); green triangles denote locations of seismographs of the HIMNT PASSCAL experiment (Schulte-Pelkum *et al.* 2005) annotated with the crustal thickness determined by simultaneous inversion of receiver function and surface wave dispersion (Priestley, unpublished results). Moho depths and earthquake focal depths are with reference to the surface.

et al. 2003; Monsalve *et al.* 2006). Monsalve *et al.* (2006) used a 27-station seismic network in eastern Nepal and the area of southern Tibet immediately to the north (Fig. 4) to locate 1649 microearthquakes. Using data from the same seismic network, Schulte-Pelkum *et al.* (2005) determined the depth to the Main Himalayan Thrust (MHT) and the Moho beneath this region. Monsalve *et al.* (2006) demonstrate that much of the seismicity occurs at shallow depths (10–20 km) in the hanging wall above the MHT but that seismicity takes place throughout the entire thickness of the 'Indian' lower crust which is underthrust beneath the MHT. They also found two zones of deeper microearthquakes: a southern cluster of events at 30–70 km depth in the epicentral region of the 1988 August 20 $M \sim 6.5$ Udayapur earthquake beneath eastern Nepal, and a northern WNW–ESE-trending zone of events at 50–100 km depth beneath the Greater Himalaya and southernmost Tibet. In these two zones the depth control provided by their local network is sufficient to show that some microearthquakes probably occur beneath the Moho, as well as in the Indian lower crust above it. The southern cluster takes place at the top of a ramp where the Indian crust bends downward to underthrust the Himalaya at a steeper dip (Schulte-Pelkum *et al.* 2005). The northern cluster occurs at the bottom of that ramp where the Indian crust flattens out beneath southern Tibet (see also Fig. 8b below).

Farther north in southcentral Tibet, Langin *et al.* (2003) used local network recordings to find that 99 per cent of the local earthquakes have focal depths of less than 25 km, and that the few apparently deeper earthquakes at 30–40 km depth had poorly constrained locations. During the operation of their network, one earthquake was reported with an apparently deeper focus based on arrival times from teleseismic data (PDE 71 km, ISC 64 km), but its actual focal depth, calculated from 41 *P*-wave and 14 *S*-wave arrival times from the local network, was 5 km.

To the east of Nepal, near 93–94°E, Kayal *et al.* (1993) and Kayal (2001) found evidence for abnormally deep continental microearthquakes in a similar tectonic environment to that of the deeper earthquakes in eastern Nepal. However, such deep microearthquakes have not been observed across the Himalayan collision zone to the west (between longitudes 75° and 85°E) (Pandey *et al.* 1999; Kayal 2001).

3.4 Summary of Indian, Himalayan and south Tibet seismicity

There is no evidence for *substantial* seismicity (in the sense of earthquakes large enough for their depths to be determined teleseismically) in the upper mantle in NW or SE Tibet. The apparently subcrustal earthquakes of Chen & Yang (2004) arise either from considering events on the fringes of the Hindu Kush deep seismic zone, plotting the event focal depths at an inappropriate location with respect to the Moho (such as projecting western Kunlun events onto the Tarim Basin Moho), or ignoring or altering the seismically determined Moho depth and using a more poorly determined Moho depth based on assumptions about gravity or topography. Moreover, there is no indication that the anomalously deep earthquakes are prevalent across all of Tibet; instead, they occur in only two regions near the NW and SE Tibetan margins, and in both places they are so close to the Moho that it is not possible to be certain on which side of it they occur. We will return to this below.

The microseismicity data of Monsalve *et al.* (2006) shows the entire thickness of the Indian crust to be seismogenic beneath the Himalaya. Subcrustal earthquakes occur in two places beneath their seismic network—at the top and bottom of a flexure or ramp where the Indian lower crust is thrust beneath the Himalaya (e.g. Fig. 8b below). These are special locations where strain rates are relatively high due to bending of the Indian Shield. As we show in the Discussion below, if the uppermost Indian mantle is sufficiently cool, some subcrustal seismicity may be expected where strain rates are high.

4 DISCUSSION

The purpose of this discussion is to use the evidence summarized so far to build up a coherent view of the structure and rheology of the Himalayan collision zone. It will then be possible to assess its significance for our general understanding of the continental lithosphere.

4.1 The Indian Shield beneath the Himalaya

The south Indian crust consists of a continuously exposed section ranging from low-grade gneisses and greenstone basins in the north to granulites in the south. With the exception of the Western Dharwar Craton and the exhumed granulite terrane, both in the far south of India, the crust of the south Indian Shield is simple and uniform (Gupta *et al.* 2003; Rai *et al.* 2003). The most important result here, as will become apparent later, is that the total crustal thickness of the eastern Dharwar craton, and by implication the crystalline crust of the northern part of the Indian Shield, is only ∼35 km, which is somewhat thin for Archean terranes. The simple structure of the crust is reflected in the simple receiver functions observed across the south Indian Shield (Rai *et al.* 2003). Receiver functions in the Himalaya and southern Tibet are much more complex, presumably because of the internal disruption of the crust as it is thickened and shortened. Rocks similar to those forming the south Indian crust may constitute the basement of the Ganges Basin and form the lower crust of the Himalaya and southern Tibet.

Beneath southernmost and NW Tibet, where the crust is thickest, these rocks should be well within the eclogite stability field. However the deep crust beneath southern Tibet cannot be predominately eclogite because the observed seismic velocities are too low to be consistent with an eclogitic lower crust. The fact that the receiver functions show a well-defined Ps conversion continuously from ∼40 km depth in northern India to ∼90 km depth in NW and SE Tibet implies that the deep crust there cannot be eclogite with a wave speed similar to that of peridotite (Christensen & Mooney 1995). For these reasons, as well as arguments related to gravity, topography and density, we agree with others (e.g. Henery *et al.* 1997; Le Pichon *et al.* 1997; Cattin *et al.* 2001; Jackson *et al.* 2004) that the deep lower crust beneath southernmost and NW Tibet is likely to be substantially metastable granulite. To be metastable the granulite must also be dry, and this dryness in turn is likely to be responsible for both the strength of the Indian Shield, manifest by its relatively large T_e (Maggi *et al.* 2000a) and its ability to produce lower-crustal earthquakes (Jackson *et al.* 2004). The receiver-function results across the Himalaya and southern Tibet support the widely held belief that as the Indian Plate underthrusts Eurasia, the upper Indian crust is folded, faulted and thickened to form the Himalaya and that the lower Indian crust underplates southern Tibet (e.g. DeCelles *et al.* 2002). The Indian and Tibetan crust are underlain by a thick, high-wave speed upper-mantle lid. Beneath southern India the base of the lid is at ∼160 km depth; beneath northern India it increases to ∼200 km depth; and beneath central Tibet it increases further to ∼250 km depth. The high-wave speed lid appears continuous across Tibet, and there is no evidence for wide-spread delamination of the lithosphere beneath Tibet.

4.2 Seismicity within the Indian Shield

The Indian Shield south of the Ganges Basin has a low level of seismicity, much of which occurs in the upper crust, but in at least some places the whole thickness of the south Indian crust is seismically active. The level of seismicity increases to the north as the Indian crust is thrust beneath the Himalaya. Most of the earthquakes occur on or above the Main Himalayan Thrust (MHT), but microearthquake studies show that the entire thickness of the Indian crustal section beneath the MHT is seismically active and that in a few places, microearthquakes may extend below the Moho where the flexure or ramp geometry of the underthrusting lower crust of India suggests that the strain rates may be particularly high. Therefore, there is no evidence in the observed seismicity in southern India for an aseismic lower crust separating a strong, seismogenic upper crust and upper mantle, and Monsalve *et al.* (2006) show clearly that microearthquakes occur throughout the entire thickness of the crust beneath the central Himalaya.

Earthquakes occur in the upper crust beneath the whole of Tibet to ∼20 km depth (e.g. Molnar & Lyon-Caen 1989) and a few earthquakes occur at 70–90 km depth beneath NW and SE Tibet, where the mid-crust is aseismic. Only in these two places is there firm evidence in the observed seismicity for two distinct seismogenic layers separated by an aseismic layer; and we examine the significance of these later. For the moment, we note that the Indian Shield itself, either south of the Himalaya or beneath it, is not a 'jelly sandwich'. It always has a single seismogenic layer, which includes the lower crust, though it can be argued that, locally, it also includes the

uppermost mantle in the region studied by Monsalve *et al.* (2006). We must now consider the significance of those microearthquakes in the mantle.

The early study of Maggi *et al.* (2000a) was faced with a problem: where there were earthquakes in the lower crust of peninsular India and parts of Africa, why were there no earthquakes in the uppermost mantle? The mantle was presumably deforming in these places, and the conventional view was that the Moho in such shield areas had a temperature of typically 300–500 °C (e.g. Artemieva & Mooney 2001). Oceanic intraplate earthquakes were thought to occur in the mantle at temperatures up to about 750 °C (e.g. Wiens & Stein 1983) and, therefore, the mantle in shields was presumably cold enough to deform seismically; yet it did not. Maggi *et al.* (2000a) speculated that small amounts of water in the continental mantle might be the possible cause. This speculation turned out to be an unnecessary complication. McKenzie *et al.* (2005) showed that the existing estimates of lithosphere geotherms in the steady-state shield areas and in the oceans were likely to be incorrect. The principal effects that required modification of conventional views were: (1) heat-producing sources in the lower crust of Archean granulite terranes were both greater and more evenly distributed than was previously thought (Jaupart *et al.* 1998; Jaupart & Mareschal 1999); (2) the crust in such regions was also often thicker, and, therefore, more heat-generating, than previously realized and (3) thermal conductivity in the mantle is a strong function of temperature, changing by a factor of two over the temperature range of the lithosphere (Schatz & Simmons 1972; Hofmeister 1999; Xu *et al.* 2004). When these factors were accounted for, geotherms could be calculated in the steady-state Precambrian shield areas that were consistent with the surface heat flow, pressure and temperature estimates from kimberlite nodule suites, and tomographic estimates of lithosphere lid thickness (McKenzie *et al.* 2005; Priestley & McKenzie 2006). In these new geotherms, the estimates of Moho temperatures in the shields were invariably up to 200 °C hotter than previously thought, and were typically around 600 °C. Furthermore, when the temperature dependence of mantle conductivity was used in oceanic plate-cooling models, it became clear that the temperature cut-off for intraplate earthquakes in oceanic mantle lithosphere was ∼600 °C (Denlinger 1992; McKenzie *et al.* 2005), not ∼750 °C as previously thought (e.g. Wiens & Stein 1983). Accordingly, a much simpler explanation for the distribution of mantle seismicity is that the mantle is seismogenic when it is colder than ∼600 °C, in both continents and oceans (McKenzie *et al.* 2005); the suggestion of Maggi *et al.* (2000a) involving water are unnecessary.

The lower continental crust is seismogenic primarily on or near the edges of shields (e.g. Foster & Jackson 1998; Maggi *et al.* 2000b; Emmerson *et al.* 2006). In these areas Moho temperatures can vary between as low as ∼500 °C (Jericho, Canadian Shield) and ∼630 °C or more (Udachnaya, Siberian Shield) (see McKenzie *et al.* 2005). The Jericho region is aseismic altogether and undeforming, whereas earthquakes in the Siberian Shield are restricted to the crust (Emmerson *et al.* 2006). As McKenzie *et al.* (2005) point out, there may be regions where seismicity extends from the lower continental crust into the mantle, if it is cool enough; such places are likely to be where the crust is thin and the earthquakes occur in Archean shields, as Moho temperatures beneath Phanerozoic orogenic belts are expected to be higher than ∼700 °C. It should be noted that, if the lower crust is seismogenic in shields where the Moho temperature is about 600 °C, then those earthquakes occur in crust much hotter than ∼350 ± 100 °C, which is the probable cut-off temperature for normal seismic activity in the 'wet' upper crust (Chen & Molnar 1983). If the crust is strong and seismogenic (large T_e and T_s) when its temperature is as high as 600 °C, it must be dry (Hirth *et al.* 1998; Mackwell *et al.* 1998; Jackson *et al.* 2004). This is the background necessary to assess the significance of the mantle microearthquakes of Monsalve *et al.* (2006) in Nepal and southernmost Tibet.

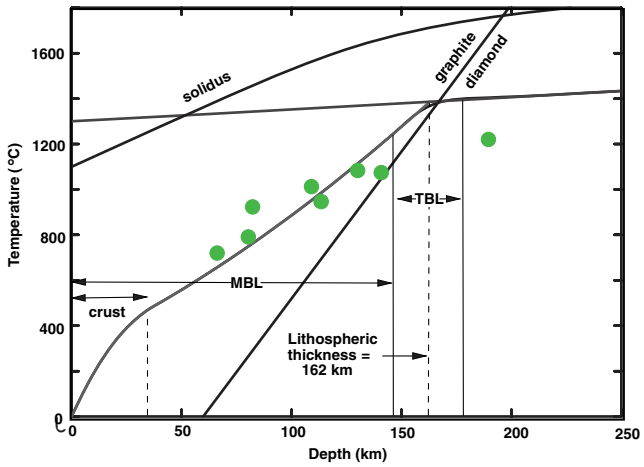

Figure 7. Steady-state geotherm of the south Indian Shield determined by fitting upper mantle xenolith data using the expressions in McKenzie *et al.* (2005). The geotherm is constrained by five data: the zero temperature at the surface, the crustal thickness, the distribution of crustal radioactivity, the pressure and temperature estimates from the xenolith, and the potential temperature of the convecting mantle. For this calculation the crust is divided into two layers, both with the same thermal conductivity, 2.5 W K^{-1} m^{-1}. The heat generation rate for the upper crust is 1.12 μW m^{-3} and the lower crust is 0.4 μW m^{-3}, values suggested by Jaupart & Mareschal (1999) for granulite. The pressure and temperature at which the mantle xenolith last equilibrated are estimated using the expressions of Brey & Kohler (1990) for the solubility of aluminium in enstatite in the presence of garnet to estimate the pressure (depth) and for the intersolubility of enstatite and diopside to obtain the temperature. The thicknesses of the upper and lower crust were varied to fit the pressure and temperature estimates from the xenolith while keeping the total crustal thickness equal to 35 km as determined from the receiver-function and surface wave-dispersion data. The heat generation in the mantle portion of the mechanical boundary layer (MBL) is taken to be zero and the thermal conductivity is taken to be a function of temperature (Schatz & Simmons 1972; Hofmeister 1999; Xu *et al.* 2004). At the base of the MBL the heat flux and temperature must be the same as those at the top of the thermal boundary layer (TBL). The temperature structure within the TBL was obtained using the expressions given by Richter & McKenzie (1981) with an interior potential temperature of 1315 °C. The xenolith data are from Ganguly & Bhattacharya (1987).

Heat flow on the Dharwar Craton is low, with a mean value of 36 m Wm^{-2} (Roy & Rao 2000). With the exception of the Western Dharwar Craton and the exhumed granulite terrane, both in the far south of India, the crust of the south Indian Shield is ∼35 km thick (Gupta *et al.* 2003; Rai *et al.* 2003). Fig. 7 shows a calculated geotherm that best fits the crustal heat generation data and upper-mantle xenolith data from the Indian Shield, using the method described by McKenzie *et al.* (2005). This geotherm gives a 162-km-thick lithosphere, in good agreement with the seismic wave speed measurement beneath southern India (Mitra *et al.* 2006a; Priestley *et al.* 2006), a Moho temperature of ∼500 °C, and a depth for the 600 °C isotherm of 57 km in a region where the crust is 35–40 km thick (Gupta *et al.* 2003; Rai *et al.* 2003). The most important influence on the estimated Moho temperature on this profile is that the crystalline crust is only about 35 km thick, thereby reducing the heat generation within it. By comparison, the crust beneath Udachnaya

in Siberia, is about 50 km thick, leading to an estimated Moho temperature of ∼630 °C.

In the context of Fig. 7 and the previous discussion, it is perhaps unsurprising that the mantle of the Indian Shield beneath the Himalaya is weakly seismogenic, as it is probably relatively cold and that, together with the increased strain-rates associated with its deforming into the ramp-and-flat geometry beneath Monsalve *et al.* (2006)'s network, may be sufficient to cause the microearthquakes. It is also no wonder that the mantle seismicity is associated with lower crustal seismicity in the same place, occurring in the strong, dry granulites of the shield left behind after formation of granites (Burton & O'Nions 1990; DeCelles *et al.* 2002). The mantle microearthquakes certainly do not represent the lower part of a 'jelly sandwich' below an aseismic lower crust.

4.3 Deep earthquakes near the Moho of SE and NW Tibet

The geotherm calculated in Fig. 7 assumes a thermal steady state, which is certainly not the case for the Indian Shield beneath Tibet. As it is underthrust northward, it is heated, mostly from above, as is clear from the thermal modelling of Cattin & Avouac (2000) and McKenzie & Priestley (2007). The thermal time constant of the lower crust of India is only a few million years, and with a horizontal underthrusting rate of ∼20 mm yr^{-1} (Zhang *et al.* 2004), the temperature structure of the incoming shield will not survive more than a few tens of km beyond the Himalayan range front (Cattin & Avouac 2000). It is thus expected that north of Monsalve *et al.* (2006)'s network, the lower crustal seismicity is lost (Molnar & Lyon-Caen 1988; Langin *et al.* 2003).

The northernmost deep earthquakes near the Moho of SE Tibet—T3, T5 and T11—(red circles in Fig. 1(c) and red focal mechanisms in Fig. 6) occur near the northern limit of the underthrusting Indian Shield, as identified by *S*-wave anisotropy (Chen & Ozalaybey 1998; Huang *et al.* 2000). Whether or not the shield is actually underthrust even further north (see DeCelles *et al.* 2002), and its heating has accounted for the change in mantle anisotropy and uppermost mantle velocity (Fig. 3c), is possible, but not clear (Priestley *et al.* 2006). Nonetheless, there is ample evidence that the mid-crust above these deep earthquakes is both hot and weak (e.g. Alsdorf & Nelson 1999). The possible significance of those earthquakes near the Moho is discussed by Jackson *et al.* (2004) who used the analogy with some high-pressure Caledonian rocks and psuedotachylites in western Norway (Austrheim 1987; Austrheim & Boundy 1994; Austrheim *et al.* 1997), to suggest that the earthquakes may be related to the infiltration of hydrous fluids and brittle fracture that accompanies a transformation of metastable granulite to eclogite. These processes, originally deduced from field geology, are supported by results of recent laboratory experiments (Green & Zhang 2006). The transformation to eclogite is accompanied by a loss of strength and further deformation of the eclogite is by ductile flow.

Thus, the situation in the region of southern Tibet north of the 'flexure' or 'ramp' (Fig. 8b) in the underthrusting Indian lower crust does indeed resemble a 'bi-modal' depth distribution of earthquakes, with some earthquakes at 80–90 km depth near the Moho and other earthquakes restricted to the top 20 km of the crust (Figs 1c and 2c). However to suggest this is confirmation of the original laminated 'jelly-sandwich' model of Chen & Molnar (1983) is misleading. The deeper earthquakes are in the Indian Shield, whether just above or just below the Moho, which has been advected beneath the overriding crust of Tibet. It is much more significant that the deep earthquakes are very close to the Moho, as the mantle is the likely source of fluids that make the granulite–eclogite transformation possible, with its accompanying loss of strength (Jackson *et al.* 2004). Furthermore, those deep earthquakes are not a universal feature of the Tibetan plateau, but occur in two very restricted areas in the SE (Fig. 6) and NW (Fig. 5). Both of these areas are about 400 km NE of the Himalayan mountain front (Fig. 8a). In the SE area, there are good reasons to think they occur in Indian Shield material (whether mantle or crust). We therefore suggest that in the NW area (Fig. 5) the deep earthquakes could also be occurring in the underthrust Indian Shield which, by implication, underlies virtually the whole of NW Tibet as far as the Altyn Tagh Fault, perhaps accounting for the step in the Moho seen by Wittlinger *et al.* (2004). If this speculation is correct, then the whole of SW Tibet could be underlain by the relatively strong Indian Shield, providing the rigid lower boundary condition that allows the mid-crust of Tibet to flow over it as a gravity current, as modelled by Copley & McKenzie (2007). In their model, it is the radially divergent mid-crustal flow of Tibet over the Indian Shield that causes the surface extension in SW Tibet, manifested by numerous normal-faulting earthquakes, not the extra elevation related to mantle delamination suggested by England & Houseman (1989), which is incompatible with observations suggesting that the Indian mantle still underlies this region.

4.4 Earthquakes and the structure of the Himalayan collision zone

The situation beneath India and southern Tibet is summarized schematically in Fig. 8(b). South of the Himalayan front, earthquakes appear to be restricted to the upper and lower crust of the Indian Shield. Earthquakes in the lower crust are likely to be in dry granulite that is capable of being seismogenic at temperatures considerably hotter than the ∼350 °C that represents the usual cut-off temperature of earthquakes in the upper granitic crust. The Moho temperature in the shield may be as low as 500 °C, largely because the crust is relatively thin (∼35 km) for an actively deforming Archean shield. As the shield is thrust beneath the Himalaya, it is bent down in a ramp-and-flat geometry (Schulte-Pelkum *et al.* 2005). At the top and bottom of this ramp the lower crust of the Indian Shield is still seismogenic, and the uppermost mantle also has the microearthquakes located by Monsalve *et al.* (2006). The mantle earthquakes, clearly rare in continental material, are probably a consequence of the low mantle temperature and the increased strain rate associated with ramp-and-flat formation. Further north, as the upper part of the lower crust warms up, earthquakes are restricted to the immediate vicinity of the Moho, while at shallower levels we see only the upper-crustal seismicity of Tibet, restricted to the top ∼20 km, giving a 'bi-modal' depth distribution which, however, has nothing to do with the original conception of Chen & Molnar (1983)'s 'jelly-sandwich' model. Meanwhile, the upper crust of India has been separated from the lower crust by low-angle thrusting and has thickened, mostly south of the IZS. The deep crustal seismicity near the Moho ceases either when the brittle granulitic blocks of the Indian lower crust are encompassed in ductile ecolgite (Jackson *et al.* 2004) or when mantle temperatures start to exceed ∼600 °C. Thus, whether or not the northern limit of the deep earthquakes in SE Tibet, at ∼32°N, which coincides with the change in anisotropic signature, is actually the northern limit of the underthrusting Indian Shield, is unclear. It is possible that it continues further north and that the internal heat generated by the very thick crust (England & Thompson 1984, 1986; Le Pichon *et al.* 1997) has raised the

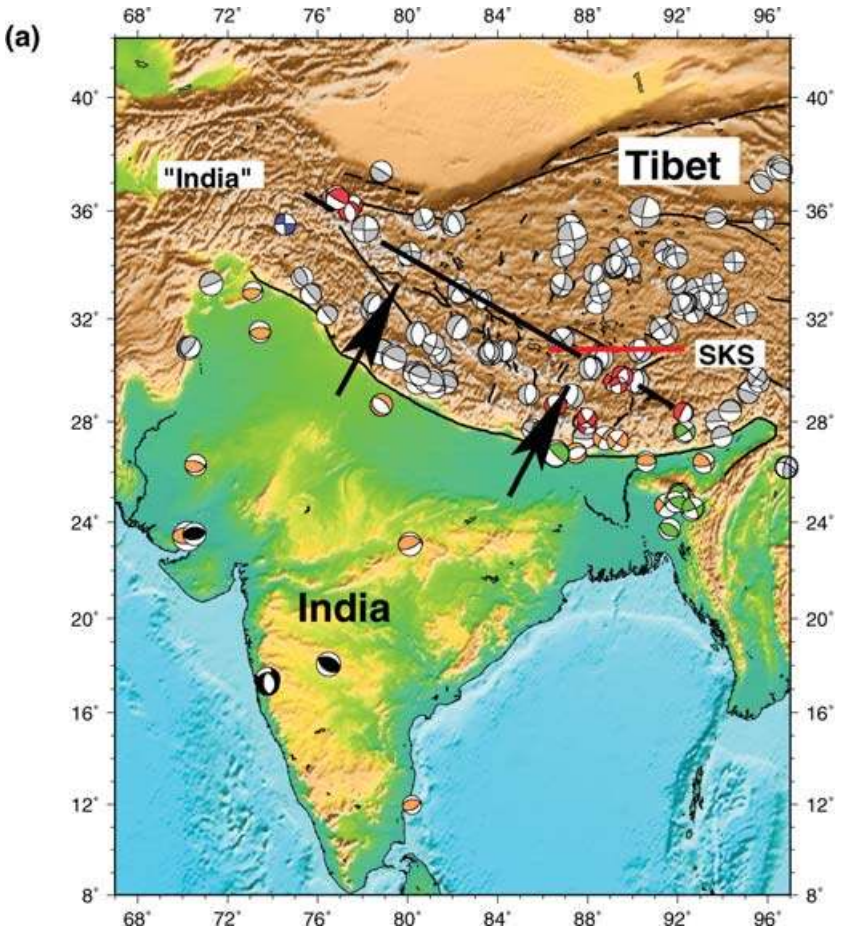

Figure 8. (a) Map of India and Tibet showing the relative motion between India and Tibet (large black arrows) and the location of the change in SKS-splitting characteristics in Tibet (red line). The locations of the transition from small SKS-splitting and weak anisotropy in the south to large SKS-splitting and strong anisotropy in the north, and the deep crustal earthquakes in NW and SE Tibet (solid black line) may mark the northern limit of India's penetration beneath Tibet or the limit of the Indian Shield as a strong entity. This might also mark the northern edge of the strong 'India' lower crust beneath south Tibet, over which the middle and upper crust of Tibet flow (Copley & McKenzie 2007). (b) Schematic cross-section from central India to central Tibet. The crystalline crust of central India is ∼35 km thick and geological observations suggest its upper part is granodiorite and its lower part is granulite (Percival *et al.* 1992). Below this, there is a high-velocity, depleted mantle layer (Priestley & McKenzie 2006). As the Indian lithosphere is thrust beneath the Himalaya, the upper Indian crust is folded, faulted and thickened to form the Himalaya and the cold, dry, strong lower granulitic crust is thrust beneath southern Tibet, thickening the Tibetan crust. The thickened Tibetan crust gradually warms due to its increased radioactivity (McKenzie & Priestley 2007). Earthquakes occur throughout the crust of central India and beneath the Himalaya; earthquakes take place in the shallow crust (< ∼20 km) throughout Tibet and in the deep crust beneath southern Tibet. As the thickened Tibetan crust heats, it forms a temperature inversion with a cool, brittle upper 'Tibetan' crust and a cool brittle lower 'Indian' crust, separated by a warm, aseismic middle crust. Earthquakes in the lower Indian crust continue to occur beneath southern Tibet until the blocks of strong granulite become isolated or until the uppermost-Indian mantle warms to ∼600 °C. As the temperature of the thick Tibetan crust increases, heat is lost upwards towards the surface and downwards into the cool, depleted upper mantle. The earthquake key is given at lower left. The black box shows the location of the HIMNT PASSCAL experiment (Schulte-Pelkum *et al.* 2005) and the ramp-and-flat shape adopted by the Indian lower crust as it thrusts beneath the Himalaya. In (b) MBT—Main Boundary Thrust, MCT—Main Central Thrust, IZS—Indus Zangpo Suture.

temperature in the uppermost mantle sufficiently to allow the *S*-wave anisotropy and velocities beneath central Tibet to change.

5 CONCLUSIONS: IMPLICATIONS FOR THE RHEOLOGY OF THE CONTINENTAL LITHOSPHERE

The original motivation for this paper was to examine the implications of the earthquake depth distribution in the Himalayan collision zone to increase our understanding of continental lithosphere rheology. As we have shown, it is possible to produce a coherent view of how the seismicity in the Himalayan collision zone is related to the lateral and vertical variations in crust and lithosphere composition, structure and temperature. None of this is in conflict with the current understanding of continental lithosphere rheology that has developed since the paper by Maggi *et al.* (2000a), and which was formulated entirely outside the Himalayan–Tibetan region. This understanding is best summarized as follows:

(i) In most continental regions, including central and northern Tibet, earthquakes are restricted to the upper crust, typically shallower than 20 km.

(ii) In some regions, the entire crustal thickness is seismogenic, down to the Moho. These are nearly all in, or on the edge of, Precambrian shields. For earthquakes to occur at the temperatures prevalent at these depths, the rocks in the lower crust are likely to be in dry granulite facies, which accounts for their strength.

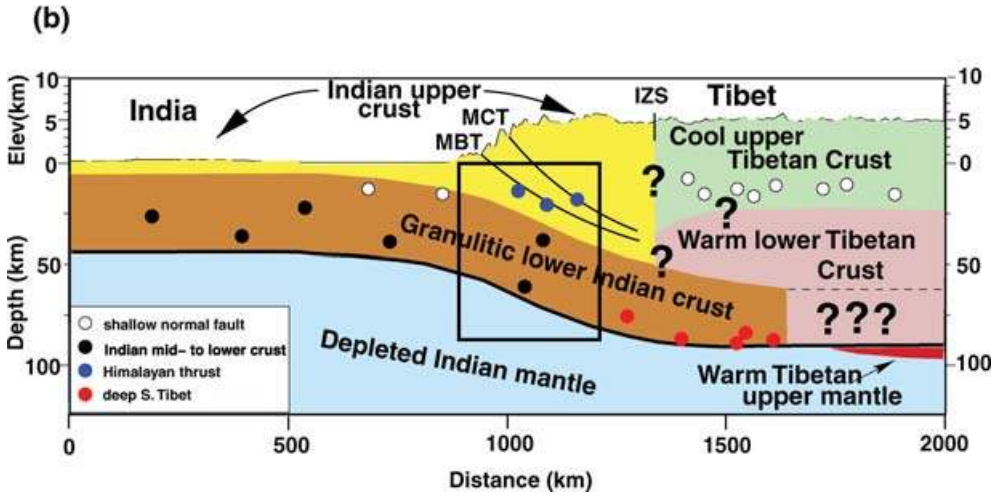

Figure 8. (*Continued.*)

(iii) Earthquakes in both the continental and oceanic mantle are restricted to material colder than ∼600 °C. On the continents, such places are likely to be rare, and include Archean shields with relatively thin crust which is undergoing deformation. This may well be the situation in northern India, beneath the Himalaya.

Most importantly, it is clearly impossible to understand the seismicity of the Himalayan collision zone without some realization that the situation is not in steady-state. What is now beneath southern Tibet was once south of the Himalaya, and has changed its temperature structure as it has underthrust northwards: it bears no direct geological relation to the rocks in the upper crust of Tibet. The deep earthquakes close to the Moho at 80–90 km beneath SE and NW Tibet, and the mantle microearthquakes beneath Nepal, are interesting curiosities. However, their contexts make clear that, contrary to the views of Chen & Yang (2004), Schulte-Pelkum *et al.* (2005) and Monsalve *et al.* (2006), they do not represent a bimodal depth distribution that vindicates the 'jelly-sandwich' model of Chen & Molnar (1983) nor do they represent a sensible peg on which to hang a generic understanding of continental rheology. The distribution of earthquake depths throughout India, Himalaya and Tibet is consistent with a generic global view of seismicity in which earthquakes occur (1) in 'wet' upper crustal material to a temperature of ∼350 °C, (2) at higher temperatures in dry granulite-facies lower crust or (3) in mantle that is colder than ∼600 °C.

ACKNOWLEDGMENTS

This research has benefited from discussions with E. Debayle, V. K. Gaur, S. Mitra, S. S. Rai and F. Tilmann. Reviews by C. Ebinger, G Hirth and an anonymous referee helped to improve the manuscript considerably. A number of the figures were prepared using Generic Mapping Tool (Wessel & Smith 1995). This is Cambridge University Department of Earth Sciences contribution ES8986.

REFERENCES

Alsdorf, D. & Nelson, K., 1999. Tibetan satellite magnetic low: evidence for widespread melt in the tibetan crust? *Geology,* **27,** 943–946.

Artemieva, I. & Mooney, W., 2001. Thermal thickness and evolution of precambrian lithosphere: a global study, *J. geophys. Res.,* **106,** 16 387–16 414.

Austrheim, H., 1987. Eclogitization of lower crustal granulites by fluid migration through shear zones, *Earth planet. Sci. Lett.,* **81,** 221–232.

Austrheim, H. & Boundy, T., 1994. Pseudotachylites generated during seismic faulting and eclogitization of the deep crust, *Science,* **265,** 82–83.

Austrheim, H., Erambert, M. & Engvik, A., 1997. Processing of crust in the root of the Caledonian continental collision zone, *Tectonophysics,* **272,** 129–153.

Bhattacharya, S., 1974. The crust-mantle structure of the Indian Peninsula from surface wave dispersion, *Geophys. J. R. astr. Soc.,* **36,** 273–283.

Bhattacharya, S., 1981. Observation and inversion of surface wave group velocities across central India, *B. Seismol. Soc. Am.,* **71,** 1489–1501.

Bodin, P. & Horton, S., 2004. Source parameters and tectonic implications of aftershocks of the m_w 7.6 Bhuj earthquake of 26 January 2001, *B. Seismol. Soc. Am.,* **94,** 818–827.

Bourjot, L. & Romanowicz, B., 1992. Crust and upper mantle tomography in Tibet using surface waves, *Geophys. Res. Lett.,* **19,** 881–884.

Brace, W. & Kohlstedt, D., 1980. Limits on lithospheric stress imposed by laboratory experiments, *J. geophys. Res.,* **85,** 6248–6252.

Brandon, C. & Romanowicz, B., 1986. A 'no-lid' zone in the central Chang-Thang platform of Tibet: evidence from pure path phase velocity measurements of long period Rayleigh waves, *J. geophys. Res.,* **91,** 6547–6564.

Brey, G. & Kohler, T., 1990. Geothermobarometry in four-phase lherzolites II. New thermobarometers, and practical assessment of existing thermobarometers, *J. Petrol.,* **311,** 1353–1378.

Burton, K. & O'Nions, R., 1990. The time scale and mechanism of granulite formation at Kurunegala, Sri Lanka, *Contrib. Miner. Petrol.,* **106,** 66–89.

Cattin, R. & Avouac, J., 2000. Modeling mountain building and the seismic cycle in the Himalaya of Nepal, *J. geophys. Res.,* **105,** 13 389–13 407.

Cattin, R., Martelet, G., Henery, P., Avouac, J., Diament, M. & Shakya, T., 2001, Gravity anomalies, crustal structure and thermo-mechanical support of the Himalaya of central Nepal, *Geophys. J. Int.,* **147,** 381–392.

Chen, W.-P., 1988. A brief update on the focal depths of intracontinental earthquakes and their correlations with heat flow and tectonic age, *Seism. Res. Lett.,* **59,** 263–272.

Chen, W.-P. & Kao, H., 1996. Seismotectonics of Asia: some recent progress, in *The Tectonic Evolution of Asia*, pp. 37–62, eds Yin, A. & Harrison, M., Cambridge University Press, Palo Alto.

Chen, W.-P. & Molnar, P., 1983. Focal depths of intracontinental and intraplate earthquakes and their implications for the thermal and mechanical properties of the lithosphere, *J. geophys. Res.,* **88,** 4183–4214.

Chen, W.-P. & Molnar, P., 1990. Source parameters of earthquakes and intraplate deformation beneath the Shillong Plateau and northern Indoburman ranges, *J. geophys. Res.,* **95,** 12 527–12 552.

Chen, W.-P. & Ozalaybey, S., 1998. Correlatio between seismic anisotropy and Bouguer gravity anomalies in Tibet and its implications for lithospheric structures, *Geophys. J. Int.,* **135,** 93–101.

Chen, W.-P. & Yang, Z., 2004. Earthquakes beneath the Himalaya and Tibet: evidence for a strong lithospheric mantle, *Science,* **304,** 1949–1952.

Chen, W.-P., Nabelek, J., Fitch, T. & Molnar, P., 1981. An intermediate depth earthquake beneath Tibet: source characteristics of the event of September 14, 1976, *J. geophys. Res.,* **86,** 2863–2876.

Christensen, N. & Mooney, W., 1995. Seismic velocity structure and composition of the continental crust—a global view, *J. geophys. Res.,* **100,** 9761–9788.

Copley, A. & McKenzie, D., 2007. Model of crustal flow in the India-Asia collision zone, *Geophys. J. Int.,* **169,** 683–698.

Curtis, A., Trampert, J., Snieder, R. & Dost, B., 1998. Eurasian fundamental mode surface wave phase velocities and their relationship with tectonic structures, *J. geophys. Res.,* **103,** 26 919–26 947.

Das Gupta, A. & Biswas, A., 2000. *Geology of Assam*, Geological Society of India, Bangalore.

DeCelles, P., Robinson, D. & Zandt, G., 2002. Implications of shortening in the himalayayn fold-thrust belt for uplift of the tibetan Plateau, *Tectonics,* **21,** 21–1–12–25, doi:10 1029/2001TC001322.

Denlinger, R., 1992. A revised estimatefor the temperature structure of the oceanic lithosphere, *J. geophys. Res.,* **97,** 7219–7222.

Dziewonski, A.M. & Anderson, D., 1981. Preliminary reference earth model, *Phys. Earth planet. Int.,* **25,** 297–356.

Ekström, G., 1987. A broad band method of earthquake analysis, *PhD thesis*, Harvard University.

Emmerson, B., Jackson, J., McKenzie, D. & Priestley, K., 2006. Seismicity, structure and rheology of the lithosphere in the Lake Baikal region, *Geophys. J. Int.,* **167,** 1233–1272.

Engdahl, E., van der Hilst, R. & Bulland, R., 1998. Global teleseismic earthquake relocation with improved travel times and procedures for depth determination, *Bull. seism. Soc. Am.,* **88,** 722–743.

England, P. & Houseman, G., 1989. Extension during continental convergence, with application to the Tibetan Plateau, *J. geophys. Res.,* **94,** 17 561–17 579.

England, P. & Thompson, A., 1984. Pressure-temperature-time paths of regional metamorphism I. Heat transfer during the evolution of regions of thickened continental crust, *J. Petrol.,* **25,** 894–928.

England, P. & Thompson, A., 1986. Some thermal and tectonic models for crustal melting in continental collision zones, in *Collision Tectonics*, Vol. 19, pp. 83–94, eds Conrad, M. & Rise, A., Geological Society, London, Special Publications.

Fan, G. & Ni, J., 1989. Source parameters of the 13 February 1980, Karakorum earthquake, *Bull. seism. Soc. Am.,* **79,** 945–954.

Foster, A. & Jackson, J., 1998. Source parameters of large African earthquakes: implications for crustal rheology and regional kinematics, *Geophys. J. Int.,* **134,** 422–448.

Ganguly, J. & Bhattacharya, P., 1987. Xenoliths in Proterozoic kimberlites from southern India: petrology and geophysical implications, in *Mantle Xenoliths*, pp. 249–265, ed. Nixson, P., Wiley and Sons, New York.

Green, H. & Zhang, J., 2006. Deformation of granulite at 1–2 GPa: Implications for deep crustal earthquakes, *EOS, Trans. Am. geophys. Un.*, **67**, Fall Meet. Suppl., MR21D-07.

Griot, D., Montagner, J. & Tapponnier, P., 1998. Phase velocity structure from Rayleigh and Love waves in Tibet and its neighboring regions, *J. geophys. Res.,* **103,** 21 215–21 232.

Gupta, S., Rai, S., Prakasham, K., Srinagesh, D., Bansal, B., Chadha, R., Priestley, K. & Gaur, V., 2003. The nature of South Indian crust: implications for Precambrian crustal evolution, *Geophys. Res. Lett.*, **30,** 1/1–4.

Henery, P., Le Pichon, X. & Goffe, B., 1997. Kinematic, thermal and petrological model of the Himalayas: constraints related to metamorphism within the underthrust Indian crust and topographic elevation, *Tectonophysics,* **273,** 31–56.

Hirth, G., Escartin, J. & Lin, J., 1998. The rheology of the lower oceanic crust: implications for lithospheric deformation of the mid-ocean ridges, in *Faultiong and Magmatism at Mid-Ocean Ridges, Geophys. Mono 106*, pp. 291–303, eds Buck, W., Delaney, P., Karson, J. & Lagabrielle, Y., *AGU,* Washington, DC.

Hofmeister, A., 1999. Mantle values of thermal condutivity and the geotherm from phonon lifetimes, *Science,* **283,** 1699–1709, doi:10.1126/science.283.5408.1699.

Houseman, G., McKenzie, D. & Molnar, P., 1981. Convective instability of a thickened boundary layer and its relavance for the thermal evolution of contimental convergent beltss, *J. geophys. Res.,* **86,** 6115–6132.

Huang, W. *et al.*, 2000. Seismic polarization anisotropy beneath the central Tibetan Plateau, *J. geophys. Res.,* **105,** 27 979–27 989.

Hwang, H.-J. & Mitchell, B., 1987. Shear velocities, q_β, and the frequency dependence of q_β in stable and tectonically active regions from surface wave observations, *Geophys. J. Int.,* **90,** 575–613.

Jackson, J., 2002a. Strength of the continental lithosphere: time to abandon the jelly sandwich?, *GSA Today,* **12,** 4–10.

Jackson, J., 2002b. Faulting, flow and the strength of the continental lithosphere, *Int. Geol. Rev.,* **44,** 39–61.

Jackson, J., Austrheim, H., McKenzie, D. & Priestley, K., 2004. Metastability, mechanical strength, and the support of mountain belts, *Geology,* **32,** 625–628.

Jaupart, C. & Mareschal, J., 1999. The thermal structure and thickness of continental roots, *Lithos,* **48,** 93–114.

Jaupart, C., Mareschal, J.C., Guillou-Frottier, L. & Davaille, A., 1998. Heat-flow and thickness of the lithosphere in the Canadian Shield, *J. geophys. Res.,* **103,** 15 269–15 286.

Julià, J., Ammon, C., Herrmann, R. & Correig, A., 2000. Joint inversion of receiver function and surface wave dispersion observations, *Geophys. J. Int.,* **143,** 99–112.

Kayal, J., 2001. Microearthquake activity in some parts of the Himalaya and the tectonic model, *Tectonophysics,* **339,** 331–351.

Kayal, J., De, R. & Chakraborty, P., 1993. Microearthquakes at the Main Boundary Thrust in eastern Himalaya and the present-day tectonic model, *Tectonophysics,* **218**(4), 375–381.

Langin, W., Brown, L. & Sandvol, E., 2003. Seismicity in central Tibet from project INDEPTH III seismic recording, *Bull. seism. Soc. Am.,* **93,** 2146–2159.

Le Pichon, X., Henery, P. & Goffe, B., 1997. Uplit of Tiet: From eclogites to granulites—implications for the Andean plateau and the Variscan belt, *Tectonophysics,* **273,** 57–76.

Ligorria, J. & Ammon, C., 1999. Iterative deconvolution and receiver-function estimation, *Bull. seism. Soc. Am.,* **89,** 1395–1400.

Mackwell, S., Zimmerman, M. & Kohlstedt, D., 1998. High-temperature deformation of dry diabase with application to tectonics on Venus, *J. geophys. Res.,* **103,** 975–985.

Maggi, A., Jackson, J., McKenzie, D. & Priestley, K., 2000a. Earthquake focal depths, effective elastic thickness, and the strength of the continental lithosphere, *Geology,* **28,** 495–498.

Maggi, A., Jackson, J., Priestley, K. & Baker, C., 2000b. A re-assessment of focal depth distribution in southern Iran, the Tien Shan and northern India: do earthquakes really occur in the continental mantle? *Geophys. J. Int.,* **143,** 629–661.

Matte, P., Mattauer, M., Olivet, J. & Griot, D., 1997. Continental subduction beneath Tibet and the Himalaya orogeny: a review, *TerraNova,* **9,** 264–270.

McKenzie, D. & Priestley, K., 2007. The influence of lithospheric thickness variations on continental evolution, *Lithos,* in press.

McKenzie, D., Jackson, J. & Priestley, K., 2005. Thermal structure of oceanic and continental lithosphere, *Earth planet. Sci. Lett.,* **233,** 337–349.

McNamara, D.E., Walter, W., Owens, T.J. & Ammon, C., 1997. Upper mantle velocity structure beneath the Tibetan Plateau from Pn travel time tomography, *J. geophys. Res.,* **102,** 493–505.

Mitra, S., Priestley, K., Bhattacharyya, A. & Gaur, V., 2005. Crustal structure and earthquake focal depths beneath northeastern India and southern Tibet, *Geophys. J. Int.,* **160,** 227–248.

Mitra, S., Priestley, K., Gaur, V. & Rai, S., 2006a. Shear-wave structure of the south Indian lithosphere from Rayleigh wave phase-velocity measurements, *Bull. seism. Soc. Am.,* **96,** 1551–1559.

Mitra, S., Priestley, K., Gaur, V., Rai, S. & Haines, J., 2006b. Variation of group velocity dispersion and seismic heterogeneity of the Indian lithosphere, *Geophys. J. Int.,* **64,** 88–98.

Molnar, P. & Chen, W.-P., 1983. Focal depths and fault plane solutions of earthquakes under the Tibetan Plateau, *J. geophys. Res.,* **88,** 1180–1196.

Molnar, P. & Lyon-Caen, H., 1988. Some physical aspects of the support, structure and evolution of mountain belts, in *Processes in Continental and Lithospheric Deformation*, Vol. 218 of Special Paper, pp. 179–207, eds J. Clark, S.P., Geological Society of America.

Molnar, P. & Lyon-Caen, H., 1989. Fault plane solutions of earthquakes and active tectonics of the Tibetan Plateau and its margins, *Geophys. J. Int.,* **99,** 123–153.

Monsalve, G., Sheehan, A., Schulte-Pelkum, V., Rajaure, S., Pandey, M. & Wu, F., 2006. Seismicity and one-dimensional velocity strcture of the Himalayan collision zone: earthquakes in the crust and upper mantle, *J. geophys. Res.,* **111,** doi:1029/2005JB004062.

Ni, J. & Barazangi, M., 1983. Hig-frequency seismic wave propagatio beneath the Indian Shield, Himilayan Arc, Tibetan Plateau and surrounding regions, high uppermost mantle velocities and different propagation beneath Tibet, *Geophys. J. R. astr. Soc.,* **72,** 665–689.

Pandey, M., Tandukar, R., Avouac, J., Vergne, J. & Heritier, T., 1999. Seismotectonics of the Nepal Himalaya from a local seismic network, *J. Aeronaut. Sci.,* **17,** 703–712.

Pegler, D. & Das, S., 1998. An enhanced image of the Pamir–Hindu Kush seismic zone from relocated earthquake hypocentres, *Geophys. J. Int.,* **134,** 573–595.

Percival, J., Fountain, D. & Salisbury, M., 1992. Exposed crustal cross sections as windows on the lower crust, in *Continental Lower Crust*, pp. 317–363, eds Fountain, D., Arculus, R. & Kay, R. Elsevier Pub., Amsterdam.

Priestley, K. & McKenzie, D., 2006. The thermal structure of the lithosphere from shear wave velocities, *Earth planet. Sci. Lett.,* **244,** 285–301.

Priestley, K., Debayle, E., McKenzie, D. & Pilidou, S., 2006. Upper mantle structure of eastern Asia from multi-mode surface waveform tomography, *J. geophys. Res.,* doi:10.1029/2005JB004082.

Rai, S., Priestley, K., Suryaprakasam, K., Srinagesh, D., Gaur, V. & Du, Z., 2003, Crustal shear velocity structure of the south Indian shield, *J. geophys. Res.,* **108**(B2), doi:10.1029/2002JB001776.

Rai, S., Priestley, K., Gaur, V., Mitra, S., Singh, M. & Searle, M., 2006. Configuration of the Indian Moho beneath the NW Himalaya and Ladakh, *Geophys. Res. Lett.,* **33,** doi:10.1029/2006GL026076.

Rao, N., Tsukuda, T., Kosuga, M., Bhatia, S. & Suresh, G., 2001. Deep lower crustal earthquakes in central India: inferences from analysis of regional broadband data of the 1997 May 21, Jabalpur earthquake, *Geophys. J. Int.,* **148,** 132–138.

Richter, F. & McKenzie, D., 1981. Parameterizations for the horizontally averaged temperature of infinite Prandtl number convection, *J. geophys. Res.,* **86,** 1738–1744.

Ritzwoller, M. & Levshin, A., 1998. Eurasian surface wave tomography: Group velocities, *J. geophys. Res.,* **103,** 4839–4878.

Romanowicz, B., 1982. Constraints on the structure of the Tibet Plateau from pure path phase velocities of L and Rayleigh waves, *J. geophys. Res.,* **87,** 6865–6883.

Roy, S. & Rao, R., 2000. Heat flow in the Indian shield, *J. geophys. Res.,* **105,** 25 587–25 604.

Schatz, J. & Simmons, G., 1972. Thermal conductivity of Earth materials at high temperatures, *J. geophys. Res.,* **77,** 6966–6983.

Schulte-Pelkum, V., Monsalve, G., Sheehan, A., Pandey, M., Sapkota, S., Bilham, R. & Wu, F., 2005. Imaging the Indian subcontinent beneath the Himalaya, *Nature,* **435,** 1222–1225, doi:10.1038/nature03678.

Tapponnier, P., Zhiqin, X., Roger, F., Meyer, B., Arnaud, N., Wittlinger, G. & Jingsui, Y., 2001. Oblique stepwise rise and growth of the Tibet Plateau, *Science,* **294,** 1671–1677.

Tilmann, F., Ni, J. & INDEPTH, III Seismic Team, 2003. Seismic imaging of the downwelling Indian lithosphere beneath central Tibet, *Science,* **300,** 1424–1427.

Wessel, P. & Smith, W., 1995. New version of the generic mapping tool release, *EOS, Trans. Am. geophys. Un.,* **76,** 329.

Wiens, D. & Stein, S., 1983. Age dependence of intraplate seismicity and implications for lithospheric evolution, *J. geophys. Res.,* **88,** 6455–6468.

Wittlinger, G., Vergne, J., Tapponnier, P., Farra, V., Poupinet, G., Jiang, M., Su, H., Herquel, G. & Paul, A., 2004. Telesesimic imaging of subducting lithosphere and Moho offsets beneath western Tibet, *Earth planet. Sci. Lett.,* **221,** 117–130.

Xu, Y., Shankland, T., Linhardt, S., Rubie, D., Langenhorst, F. & Klasinski, K., 2004. Thermal diffusivity and conductivity of olivine, wadsleyite and ringwoodite to 20 GPa and 1373 K, *Phys. Earth planet. Int.,* **143,** 321–336, doi:10.1016/j.pepi.2004.03.005.

Yuan, X., Ni, J., Kind, R., Mechie, J. & Sandvol, E., 1997. Lithospheric and upper mantle structure of southern Tibet from a seismological passive source experiment, *J. geophys. Res.,* **102,** 27 491–27 500.

Zhang, P.-Z. *et al.*, 2004. Continuous deformation of the Tibetan Plateau from global positioning system data, *Geology,* **32,** 809–812.

Zhou, H. & Murphy, M., 2005. Tomographic evidence for wholesale underthrusting of India beneath the entire Tibetan plateau, *J. Aeronaut. Sci.,* **25,** 445–457.

Zhu, L. & Helmberger, D., 1996. Intermediate depth earthquakes beneath the India–Tibet collision, *Geophys. Res. Lett.,* **23,** 435–438.